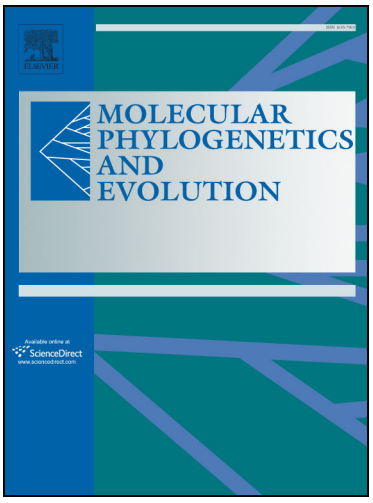

Cross-contamination and strong mitonuclear discordance in *Empria* sawflies (Hymenoptera, Tenthredinidae) in the light of phylogenomic data

Marko Prous, Kyung Min Lee, Marko Mutanen

PII: S1055-7903(19)30042-9
DOI: https://doi.org/10.1016/j.ympev.2019.106670
Reference: YMPEV 106670

To appear in: *Molecular Phylogenetics and Evolution*

Received Date: 21 January 2019
Revised Date: 2 November 2019
Accepted Date: 4 November 2019

Please cite this article as: Prous, M., Min Lee, K., Mutanen, M., Cross-contamination and strong mitonuclear discordance in *Empria* sawflies (Hymenoptera, Tenthredinidae) in the light of phylogenomic data, *Molecular Phylogenetics and Evolution* (2019), doi: https://doi.org/10.1016/j.ympev.2019.106670

Cross-contamination and strong mitonuclear discordance in *Empria* sawflies (Hymenoptera, Tenthredinidae) in the light of phylogenomic data

Marko Prous[a,b,*, #], Kyung Min Lee[c,#], Marko Mutanen[c]

[a] Senckenberg Deutsches Entomologisches Institut, Eberswalder Straße 90, 15374 Müncheberg, Germany
[b] Department of Zoology, Institute of Ecology and Earth Sciences, University of Tartu, Vanemuise 46, 51014, Tartu, Estonia
[c] Ecology and Genetics Research Unit, University of Oulu, PO Box 3000, FI-90014, University of Oulu, Finland

[*] Corresponding author at: Senckenberg Deutsches Entomologisches Institut, Eberswalder Straße 90, 15374 Müncheberg, Germany
E-mail address: mprous@senckenberg.de (M. Prous)

[#] Joint first authorship.

Keywords:
COI barcoding
ddRAD sequencing
DNA barcode sharing
Phylogenomics
Species delimitation

Abstract

In several sawfly taxa strong mitonuclear discordance has been observed, with nuclear genes supporting species assignments based on morphology, whereas the barcode region of the mitochondrial COI gene suggests different relationships. As previous studies were based on only a few nuclear genes, the causes and the degree of mitonuclear discordance remain ambiguous. Here, we obtained genomic-scale ddRAD data together with Sanger sequences of mitochondrial COI and two to three nuclear protein coding genes to investigate species limits and mitonuclear discordance in two closely related species groups of the sawfly genus *Empria*. As found previously based on nuclear ITS and mitochondrial COI sequences, species are in most cases supported as monophyletic based on ~~previous and~~ new nuclear data reported here, but not based on mitochondrial COI. This mitonuclear discordance can be explained by occasional mitochondrial introgression with little or no nuclear gene flow, a pattern that might be common in haplodiploid taxa with slowly evolving mitochondrial genomes. Some species in the *E. immersa* group are not recovered as monophyletic according to either mitochondrial or nuclear data, but this could partly be because of unresolved taxonomy. Preliminary analyses of ddRAD data did not recover monophyly of *E. japonica* within the *E. longicornis* group (three Sanger sequenced nuclear genes strongly supported monophyly), but closer examination of the data and additional Sanger sequencing suggested that both specimens were substantially (possibly 10–20% of recovered loci) cross-contaminated. A reason could be specimen identification tag jumps during sequencing library preparation that in previous studies have been shown to affect up to 2.5% of the sequenced reads. We provide an R script to examine patterns of identical loci among the specimens and estimate that the cross-contamination rate is not unusually high for our ddRAD dataset as a whole (based on counting of identical sequences in the *immersa* and *longicornis* groups, which are well separated from each other and probably do not hybridise). The high rate of cross-contamination for both *E. japonica* specimens might be explained

by the small number of recovered loci (~1000) compared to most other specimens (>10 000 in some cases) because of poor sequencing results. We caution against drawing unexpected biological conclusions when closely related specimens are pooled before sequencing and tagged only at one end of the molecule or at both ends using a unique combination of limited number of tags (less than the number of specimens).

1. Introduction

Continuing advances in high-throughput sequencing technologies and falling prices make it increasingly easier to collect genome-scale data for many non-model organisms. The large amount of data that could be obtained with high-throughput next generation sequencing methods makes it possible to answer many biological questions simultaneously (in phylogeny, population genetics, evolutionary ecology etc.) and in higher resolution than would be possible with more traditional methods (e.g. Sanger sequencing of one or few markers, genotyping by microsatellites etc.). However, the large amount of data that is generated with next generation sequencing methods introduces its own problems that are hardly relevant when only few markers are analysed. Genome-scale or phylogenomic datasets are plagued mainly by two types of errors: data errors and systematic errors (Philippe et al., 2017). Data errors, such as assembly and alignment artefacts or contaminants, for example, are easy to control ~~for~~ in single-gene scale datasets, but prohibitive in genome-scale datasets if checked manually. Because automated methods of dataset assembly are not (yet) perfect, some data errors are nearly always introduced in phylogenomic datasets. Even if the dataset is perfectly assembled (all contaminants and non-homologous alignments excluded), one still has to consider systematic errors (e.g. biases in nucleotide or amino acid composition, unequal rates of evolution) which only increase with dataset size and therefore could seriously mislead phylogenomic analyses, although this problem becomes critical only when dealing with ancient divergences (tens and more millions of years ago) (Philippe et al., 2017, 2005; Tarver et al., 2016).

DNA barcoding of single molecular marker for the purpose of species identification can also benefit from high-throughput sequencing, as hundreds or thousands individuals could be sequenced simultaneously (e.g. Cruaud et al., 2017; Hebert et al., 2018; Meier et al., 2016). For animals, a ~650 bp fragment from 5' end of the mitochondrial cytochrome c oxidase I (COI) has been chosen as the standard barcoding marker (Hebert et al., 2003), which by now has been sequenced from more than five million individuals according to the Barcode of Life (BOLD) database (www.boldsystems.org). Although this short mitochondrial fragment seems to be suitable in most species rich groups, such as Coleoptera and Lepidoptera (Mutanen et al., 2016; Pentinsaari et al., 2017; Zahiri et al., 2017), rampant mitochondrial introgression is also known in some groups (Sloan et al., 2017). In some cases the usefulness of COI sequences is not clear due to lack of sequencing efforts and / or taxonomic research. For example, while large-scale COI sequencing efforts have been applied also to many hyperdiverse insect groups, congruence with sufficiently informative nuclear genes and / or morpho-taxonomy has not always been evaluated (Alex Smith et al., 2013; Hebert et al., 2016). Nevertheless, some theoretical considerations ~~can~~ give indications in which cases mitonuclear discordances could be expected at an increased rate (Ivanov et al., 2018; Sloan et al., 2017). Particularly, Patten et al. (2015) found recently through theoretical modelling that haplodiploid species may be especially prone to biased mitochondrial introgression, which could be amplified by several other adaptive and non-adaptive conditions (reviewed by Sloan et al., 2017). The most species rich group (at least in terms of described species) of haplodiploid animals is Hymenoptera (sawflies, ants, bees, and wasps) and could therefore be a good candidate for investigating mitochondrial introgression and utility of mitochondrial barcodes. Besides haplodiploidy, mutation rate of mitochondrial DNA (mtDNA) could also be a factor affecting rate of mitochondrial introgression. Sloan et al. (2017) suggested that lower mutation rates promote

adaptive mitochondrial introgression while higher rates lead more likely to compensatory co-evolution and mitonuclear incompatibilities. As mitochondrial genomes of Apocrita (the bulk of hymenopteran species) evolve faster than those of basal hymenopterans (Kaltenpoth et al., 2012; Ma et al., 2019; Niu et al., 2019; Tang et al., 2019), mitochondrial introgression might be less common in Apocrita compared to sawflies. Within the sawflies, Xyeloidea, Pamphilioidea, and Tenthredinoidea have the slowest evolving mtDNA, while Cephoidea, Orussoidea, Siricoidea, and possibly Anaxyleoidea (which are more closely related to Apocrita), have an intermediate or fast evolutionary rate (Ma et al., 2019; Niu et al., 2019; Tang et al., 2019). While we are not aware of cases of large-scale discordance between mitochondrial barcodes and species boundaries in Apocrita, there are several such cases among sawflies, particularly among Tenthredinoidea (Linnen and Farrell, 2007; Schmidt et al., 2017). However, in all those cases discordances were identified based on morphology and COI barcodes, or morphology plus few nuclear genes and COI barcodes, and it is likely that in some cases operational factors, such as over-splitting of species, are involved too (cf. Mutanen et al., 2016).

Here we investigate based on genome-scale data the phylogeny and species limits in two closely related species groups (divergence probably not more than few million years) within the sawfly genus *Empria* Lepeletier & Serville, 1828 (Hymenoptera, Tenthredinidae). The genus includes at least 60 species, several of which are still undescribed (Prous, 2012). Most species in the genus are externally rather similar to each other, which makes species identification difficult. However, the differences in the structure of ovipositors and penis valves are often very clear even between closely related species (Prous, 2012).

Taxonomic and limited phylogenetic studies on the genus have revealed two species complexes (*longicornis* and *immersa* groups) where species delimitation has been especially problematic (Prous, 2012; Prous et al., 2014, 2011b). Based on morphology, the main evidence in both of the groups indicating the presence of more than one species, is the structure of the female ovipositor, which often shows clear differences between species and which correlates with host plant use (Prous, 2012; Prous et al., 2011b). Species in the *longicornis* group specialise on different herbaceous genera in Rosaceae (specifically in subfamily Rosoideae and genus *Dryas*) and species in the *immersa* group on *Betula* or *Salix*. Differences in other morphological characters (including male genitalia) are rather weak between the species, but can nevertheless be helpful in species identification. While sequencing of mitochondrial COI gene did not reveal any correlation with species boundaries defined using ~~on~~ morphological and ecological data, nuclear ITS (internal transcribed spacers 1 and 2) sequence data did (Prous, 2012; Prous et al., 2011b). Discord between mitochondrial and morphological plus nuclear ITS data in these groups is quite remarkable: different species frequently have identical COI barcodes (658 bp) or even complete (1536 bp) COI gene (Prous et al., 2011b), while at the same time different specimens of the same species can diverge by 3.3% in the barcoding region. To better understand this discord and to test species boundaries in the *longicornis* and *immersa* groups, we collected genome-wide data using double digest RADseq (Lee et al., 2018; Peterson et al., 2012) and sequenced long fragments of two to three nuclear protein coding genes.

Results showed that in some cases there was substantial cross-contamination in RADseq data, which might have escaped detection without the knowledge of the organisms involved (based on morphological, ecological and single gene data) and initial manual checks. This cross-contamination had significant impact on the phylogenetic tree building and population admixture analyses. We developed a workflow to detect possible cases of cross-contamination and exclude these from downstream analyses.

2. Materials and methods

2.1. DNA extraction

For most specimens, DNA was extracted as described in Prous et al. (2011b). New DNA extractions for this study were obtained with an EZNA Tissue DNA Kit (Omega Bio-tek) according to the manufacturer's protocol and stored at -20 °C for later use. Typically, the middle right leg was used for DNA extraction, but for males the whole genital capsule was often additionally used to increase DNA yield and to free penis valves from muscles for photography. Specimens that were selected for sequencing are listed in Table 1.

Table 1. Collection data of *Empria* specimens selected for sequencing. CMH – Private collection of Mikk Heidemaa (Tartu, Estonia); DEI - Senckenberg Deutsches Entomologisches Institut, Müncheberg, Germany; ISEA - Institute of Systematics and Ecology of Animals, Russian Academy of Sciences, Novosibirsk, Russia; IZBE - Estonian University of Life Sciences, Tartu, Estonia; LOENNV - Private collection Ole Lønnve, Oslo, Norway; TUZ - University of Tartu, Tartu, Estonia; UOG - University of Guelph, Guelph, Canada; USNM - Smithsonian Institution, National Museum of Natural History, Washington DC, USA; ZIN - Zoological Institute, Russian Academy of Sciences, Saint Petersburg, Russia.

Specimen ID	Group	Species	Sex	Country	Decimal coordinates	Collecting date	Collected by	Collection
DEI-GISHym20706	immersa	E. camtschatica	male	Sweden	62.435N 13.835E	2013-06-07	Liston, Prous & Taeger	DEI
DEI-GISHym80070	immersa	E. camtschatica	female	Sweden	67.212N 23.497E	2014-06-10	A. Taeger	DEI
BIOUG00998-E05	immersa	E. fletcheri	male	Canada	58.754N 93.997W	2010-06-17	J. Wang	UOG
BIOUG17274-F06	immersa	E. fletcheri	male	Canada	60.714N 137.432W	2014-07-02	C. Wong	UOG
DEI-GISHym31039	immersa	E. fletcheri	male	Sweden	66.035N 22.16E	2014-05-28	A. Liston & M. Prous	DEI
TUZ615113	immersa	E. fletcheri	male	UK	56.99237N 3.50222W	2010-06-04	M. Prous	TUZ
TUZ615334	immersa	E. fletcheri	male	Estonia	59.1028N 25.4983E	2011-05-22	M. Prous	TUZ
DEI-GISHym80045	immersa	E. immersa	male	Sweden	66.166N 23.495E	2014-06-01	A. Liston & M. Prous	DEI
DEI-GISHym80071	immersa	E. immersa	male	Sweden	66.534N 19.721E	2014-06-11	A. Taeger	DEI
TUZ615623	immersa	E. immersa	male	Finland	65.078N 25.482E	2012-06-22	M. Prous	TUZ
BIOUG00998-B05	immersa	E. improba	female	Canada	58.626N 94.229W	2010-06-16	J. Wang	UOG
BIOUG00998-D05	immersa	E. improba	male	Canada	58.626N 94.229W	2010-06-13	J. Wang	UOG
BIOUG00998-D06	immersa	E. improba	female	Canada	58.626N 94.229W	2010-06-13	J. Wang	UOG
BIOUG00998-C05	immersa	E. plana	male	Canada	58.754N 93.997W	2010-06-28	J. Wang	UOG
DEI-GISHym15478	immersa	E. plana	female	Sweden	62.435N 13.835E	2013-06-07	Liston, Prous & Taeger	DEI
TUZ615181	immersa	E. plana	female	Japan	43.4166N 142.68066E	2009-06-24	A. Shinohara	TUZ
DEI-GISHym80142	longicornis	E. alector	male	Germany	48.908N 10.008E	2016-05-07	SDEI	DEI
TUZ615036	longicornis	E. alector	male	Estonia	57.774N 26.339E	2008-05-03	M. Prous	TUZ
TUZ615121	longicornis	E. alector	male	Estonia	59.22889N 25.31694E	2009-05-17	M. Prous	TUZ
TUZ615220	longicornis	E. alector	female	Estonia	58.884N 22.636E	2008-05-31	M. Prous	TUZ
DEI-GISHym15214	longicornis	E. alpina	male	Sweden	68.362N 18.723E	2012-07-05	A.D. Liston & A. Taeger	DEI
DEI-GISHym80011	longicornis	E. alpina	male	Russia	52.80771N 93.28815E	2011-06-20	E. V. Borisova	ISEA
DEI-GISHym80106	longicornis	E. alpina	male	Sweden	68.409N 18.639E	2016-07-01	A. Liston & M. Prous	DEI
DEI-GISHym14890	longicornis	E. basalis	female	Slovakia	48.9695N 19.65E	2005-06-22	A. Taeger	DEI
OL10-02	longicornis	E. basalis	male	Norway	59.95N 9.03333E	2010-05-24/2010-07-14	O. Lonnve	LOENNV

TUZ615083	longicornis	E. basalis	female	Estonia	57.653N 26.242E	2008-05-03	M. Prous	TUZ
TUZ615141	longicornis	E. basalis	male	UK	56.5253N 4.2911W	2010-06-05	M. Prous	TUZ
TUZ615625	longicornis	E. basalis	female	Finland	65.0775N 25.4915E	2012-06-22	M. Prous	TUZ
TUZ615162	longicornis	E. japonica	female	Japan	43.647N 142.791E	2008-06-22	A. Shinohara	TUZ
USNM2051678_003	longicornis	E. japonica	male	Japan	43.6667N 143.1E	2008-06-06/2008-06-27	A. Ueda	USNM
USNM2051678_038	longicornis	E. japonica	male	Japan	43.6667N 143.1E	2008-06-06/2008-06-27	A. Ueda	USNM
TUZ615180	longicornis	E. loktini	female	Japan	43.647N 142.791E	2008-06-22	A. Shinohara	TUZ
DEI-GISHym14886	longicornis	E. longicornis	male	Slovakia	49.01183N 19.823E	2005-06-19	A. Taeger	DEI
TUZ615022	longicornis	E. longicornis	male	France	45.587N 2.824E	2008-05-22	M. Prous	TUZ
TUZ615057	longicornis	E. longicornis	larva [b]	Estonia	58.444N 26.653E	2006-05-25	M. Prous	TUZ
DEI-GISHym21189	longicornis	E. minuta	female	Sweden	65.82N 24.033E	2014-06-03	A. Liston & M. Prous	DEI
IZBE0350001	longicornis	E. minuta	male	Estonia	58.329N 26.94E	2009-04-19/2009-05-02	O. Kurina	IZBE
MH10-01	longicornis	E. minuta	male	Estonia	58.41N 26.5511E	2010-04-12/2010-04-30	M. Heidemaa	CMH
DEI-GISHym80040	longicornis	E. montana	male	Russia	52.80771N 93.28815E	2011-06-20	E. V. Borisova	ISEA
ZIN_Hym_1796001 [a]	longicornis	E. montana	male	Russia	61.9N 149.5E	1987-07-09/1987-07-15	A. Zinovjev	ZIN
ZIN_Hym_1796002 [a]	longicornis	E. montana	female	Russia	61.9N 149.5E	1987-07-09/1987-07-15	A. Zinovjev	ZIN
USNM2051678_040	longicornis	E. sp11	male	Japan	43.6667N 143.1E	2008-06-06/2008-06-27	A. Ueda	USNM
DEI-GISHym15231	longicornis	E. sp14	female	Austria	47.52299N 13.69299E	2011-06-30	Blank, Liston & Taeger	DEI
MH11-01	longicornis	E. sp14	male	France	42.74333N 0.09339E	2011-05-28	M. Heidemaa	CMH
DEI-GISHym20872	longicornis	E. tridens	larva	Germany	49.61689N 7.91258E	2013-07-05	K. Bähner	DEI
TUZ615023	longicornis	E. tridens	larva [b]	Estonia	58.483N 26.483E	2007-05-13	M. Prous	TUZ
TUZ615027	longicornis	E. tridens	larva [b]	Estonia	59.208N 25.571E	2006-05-07	M. Prous	TUZ
TUZ615037	longicornis	E. tridens	male	France	45.587N 2.824E	2008-05-22	M. Prous	TUZ
TUZ615165	longicornis	E. tridens	male	Switzerland	46.091N 9.013E	2009-05-27	M. Prous	TUZ
TUZ615624	longicornis	E. tridens	male	Finland	65.078N 25.482E	2012-06-22	M. Prous	TUZ
USNM2057434_19	longicornis	E. tridens	male	Japan	43.0667N 142.6833E	2009-06-05/2009-06-25	A. Ueda	USNM
DEI-GISHym86125 [a]	outgroup	E. gelida	female	Russia	43.694N 132.168E	2016-05-19	Kramp, Prous & Taeger	DEI
TUZ615182	outgroup	E. tridentis	male	Japan	43.647N 142.791E	2008-06-22	A. Shinohara	TUZ

[a] – For these specimens no attempt to obtain ddRAD data was made.

[b] – Collecting data is of the female, from which the larva was reared.

2.2. Sanger sequencing

To test congruence between mitochondrial and nuclear gene trees and to compare results based on Sanger sequencing of small number of genes with the genome-scale ddRAD sequencing, we initially amplified fragments of three genes, one mitochondrial and two nuclear. The mitochondrial gene used is a complete (amplified and sequenced as described in Prous et al., 2011b) or partial cytochrome oxidase subunit I (COI). For most specimens, the sequenced fragment is at least 1078 bp. One specimen (BIOUG00998-B05, GenBank accession JX830389) had only the 658 bp fragment corresponding to the standard barcode region of the animal kingdom (Hebert et al., 2003). Complete or partial COI barcode sequences of three specimens (BIOUG17274-F06, BIOUG00998-D06, BIOUG00998-B05) were available in BOLD (http://www.boldsystems.org/), two of which were extended to 1078 bp by doing new DNA extractions, amplifications, and sequencing. The two nuclear markers are fragments of sodium/potassium-transporting ATPase subunit alpha (NaK) and DNA dependent RNA polymerase II subunit RPB1 (POL2). The NaK fragment used is a nearly complete sequence of its longest exon, 1654 bp. The POL2 fragment used is composed of two partial exons and one short intron that did not vary in length (87 bp) in the specimens studied here, altogether 2494–2710 bp, depending on the primer set used. After the first analyses of ddRAD data, we suspected cross-contamination in *Empria japonica*. To test this, we selected two variable candidate RAD loci that we suspected to be contaminated in *E. japonica* and designed primers to amplify and re-sequence these regions. One of the selected loci turned out to be a fragment of the zinc finger CCCH domain-containing protein 14 (ZC3H14) for which we designed additional primers to amplify its longest exon (containing also the ddRAD locus), varying between 1582–1639 bp in the studied specimens. For the second candidate locus (anonymous), quite a similar (around 80%) match was found only among the WGS (whole genome shotgun) contigs of *Neodiprion lecontei* (scaffold_346, GenBank accession LGIB01000346). This locus might be non-coding because of apparent frame-shifting indels in some ddRAD sequences, but was of the same length in the PCR amplified specimens, 138 bp. Primers used for amplification and sequencing are listed in Table 2. New POL2 and ZC3H14 primers (Table 2) were designed based on WGS contigs of four sawfly genomes (GenBank accessions AOFN01001568, LGIB01000323, AMWH01001469, AZGP01005167, AOFN02000929, LGIB01000132, AMWH01002139, AZGP02000664), sawfly transcriptomes published by Misof et al. (2014) and Peters et al. (2017), and based on POL2 sequences published by Malm and Nyman (2015). Numbers in the new POL2 and ZC3H14 primer names refer to the binding position of the primer's 3' end in the coding region of *Athalia rosae* mRNA (accessions XM_012395805 and XM_012401276). Primers for the anonymous locus were designed based on our ddRAD data.

PCR reactions were carried out in a total volume of 15–30 µl containing 1–2 µl of extracted DNA, 1.0–3.0 µl (5.0–15 pmol) of primers and 7.5–15 µl of 2x Multiplex PCR Plus Master mix (QIAGEN). The PCR protocol consisted of an initial DNA polymerase (HotStar Taq) activation step at 95 °C for 5 min, followed by 38–40 cycles of 30 s at 95 °C, 90 s at 49–59 °C depending on the primer set used, and 60–180 s (depending on the amplicon size) at 72 °C; the last cycle was followed by a final 30 min extension step at 68 °C. 3 µl of PCR product was visualised on a 1.4% agarose gel and then purified with FastAP and Exonuclease I (Thermo Scientific). 1.0–2.0 U of both enzymes were added to 12–27 µl of PCR solution and incubated for 15 min at 37 °C, followed by 15 min at 85 °C. 3–5 µl of purified PCR product per primer in a total volume of 10 µl (5–7 µl of sequencing primer at concentration 5 pmol/µl) were sent to Macrogen (Netherlands) for sequencing. Ambiguous positions (i.e. double peaks in chromatograms) due to heterozygosity or heteroplasmy were coded using IUPAC symbols. Sequences reported here have been deposited in the GenBank (NCBI) database (accession numbers MK299849–MK299982).

Table 2. Primers used for PCR and sequencing (preferred primers in bold), with information provided on respective gene fragment, primer name, direction (forward, F or reverse, R), primer sequence, standard PCR annealing temperature, utilization (PCR/ sequencing), and reference. Primer annealing temperatures used for sequencing at Macrogen were 47°C for COI and 50°C for nuclear genes.

Gene Region	Primer name	F/ R	Primer sequence 5′–3′	PCR annealing temperature (°)	PCR/ Sequencing	Reference
COI	**SymF1**	F	TTTCAACWAATCATAAARAYATTGG	47	PCR, seq	(Prous et al., 2016)
COI	**Sym-C1-J1718**	F	GGAGGATTTGGAAAYTGAYTAGTWCC	49	PCR, seq	(Nyman et al., 2006)
COI	**symC1-J1751**	F	GGAGCNCCTGATATAGCWTTYCC	47	Seq	(Prous et al., 2016)
COI	**SymR1**	R	TAAACTTCWGGRTGICCAAARAATC	47	PCR, seq	(Prous et al., 2016)
COI	SymR2	R	TAAACTTCTGGRTGTCCAAARAATCA	47	PCR, seq	(Prous et al., 2016)
COI	**A2590**	R	GCTCCTATTGATARWACATARTGRAAATG	49	PCR, seq	(Normark et al., 1999)
NaK	**NaK_263F**	F	CTYAGCCAYGCRAARGCRAARGA	59	PCR, seq	(Prous et al., 2017)
NaK	**NaK_809F**	F	GCWTTYTTCTCNACSAAYGCSGTNGARGG	55	PCR, seq	(Prous et al., 2017)
NaK	**NaK_907Ri**	R	TGRATRAARTGRTGRATYTCYTTIGC	54	PCR, seq	(Prous et al., 2017)
NaK	NaK_910R	R	TGRATRAARTGRTGRATYTCYTT	50	PCR, seq	(Prous et al., 2017)
NaK	**NaK_1250Fi**	F	ATGTGGTTYGAYAAYCARATYATIGA	56	PCR, seq	(Prous et al., 2017)
NaK	**NaKRev475**	R	TCGATRATYTGRTTRTCRAACCACAT	56	seq	(Leppänen et al., 2012)
NaK	**NaK_1498R**	R	ACYTGRTAYTTGTTNGTNGARTTRAA	52	PCR, seq	This study
NaK	**NaK_1918R**	R	GATTTGGCAATNGCTTTGGCAGTDAT	59	PCR, seq	(Prous et al., 2017)
POL2	POL2_104Fi	F	GYATGTCAGTYACNGATGGIGG	59	PCR, seq	This study
POL2	**POL2_104Fv2**	F	CGNATGTCNGTNACNGAYGGIGG	60	PCR, seq	This study
POL2	**POL2_574R**	R	TCYTCRTTNACRTGYTTCCAYTCNGC	59	seq	This study
POL2	POL2_599F	F	GARTGGAARCAYGTVAAYGARGA	54	PCR, seq	This study
POL2	**POL2_797F**	F	ATGTAYGGNTCNGCNAARAAYCARGA	58	PCR, seq	This study
POL2	POL2_889R	R	TGRAAYTGYARCATYTTWATRTTYTC	52	PCR, seq	This study
POL2	**POL2_928R**	R	GGCATNCCNGGCATRTCRTTRTCNAC	59	PCR, seq	This study
POL2	**POL2_1388F**	F	CAYAARATGAGTATGATGGG	51	PCR, seq	This study
POL2	POL2_1459R	R	TTCATYTCRTCNCCRTCRAARTC	52	PCR, seq	This study

POL2	**POL2_1706F**	F	TGGGAYGGNAARATGCCNCARCC	60	PCR, seq	This study
POL2	POL2_1759R	R	ATCATRTTNACRTTNCCNGGDATDAT	55	PCR, seq	This study
POL2	**POL2_1777Ri**	R	GTRCTGTGIGTYCKDATCATRTT	55	PCR, seq	This study
POL2	POL2 hym 3F	F	ACNCACAGYACNCAYCCNGAYGA	56	Seq	(Malm and Nyman, 2015)
POL2	POL2_2423F	F	CATTTYATHAARGAYGAYTAYGG	51	Seq	This study
POL2	**POL2_2509R**	R	TTNACRGCRGTATCRATNAGACCYTC	60	PCR, seq	This study
POL2	POL2_2725R	R	GGATCRAAYTTRAAYTTYTTYTC	50	PCR, seq	This study
ZC3H14	**ZC3H14_59F**	F	TAGAGYGCNATYCGNGCNAARCT	58	PCR, seq	This study
ZC3H14	**ZC3H14_212F**	F	TTYGTNGANTGGCTNCAYGAYCARGT	60	Seq	This study
ZC3H14	**ZC3H14_838R**	R	ATYCTNGGYTTRTTNACRCTNGAYTT	55	PCR, seq	This study
ZC3H14	**ZC3H14_863F**	F	AARTCNAGYGTNAAYAARCCNAGRAT	55	PCR, seq	This study
ZC3H14	**ZC3H14_1696R**	R	GGYCTNGGNGTNACDATNACYTTRCT	60	Seq	This study
ZC3H14	**ZC3H14_1780R**	R	ACVACNGAYTGRTTNGCYTCNGCRAC	60	PCR, seq	This study
anonymous	Nlec346F	F	ACACGTGATCAATAATAACGACT	55	PCR, seq	This study
anonymous	Nlec346R	R	ATCGTACAATGATTCGGGACTAT	55	PCR, seq	This study

2.3. ddRADseq library preparation and bioinformatics

The quantity of genomic DNA (gDNA) was checked using PicoGreen kit (Molecular Probes). To obtain sufficient quality and quantity of gDNA from the low concentrations available, whole genome amplification was performed using REPLI-g Mini kit (Qiagen). The ddRADseq library was implemented following protocols described in (Lee et al., 2018) with one exception: the size distribution and concentration of the pools were measured with Bioanalyzer (Agilent Technologies). The de-multiplexed *Empria* fastq data are archived in the NCBI SRA: PRJNA505249 (Lee, 2018).

Raw paired-end reads were demultiplexed with no mismatches tolerated using their unique barcode and adapter sequences using *ipyrad* v.0.7.23 (Eaton and Overcast, 2016). All *ipyrad* defaults were used, with the following exceptions: the minimum depth at which majority rule base calls are made was set to 3, the clustering threshold was set to 0.95, the minimum number of samples that must have data at a given locus for the locus to be retained was set to 4, and the assembly method was set to denovo and reference for independent testing. The reference assembly method is based on mapped reads to *Athalia rosae* genome sequences (GenBank, GCA_000344095) with BWA using the default bwa-mem setting (Li, 2013) based on 95% of sequence similarity.

2.4. Phylogenetic analysis

Maximum likelihood (ML) trees were inferred in RAxML v.8.2.0 or v8.2.10 (Stamatakis, 2014), with bootstrap support estimated by a 1,000 replicates rapid bootstrap analysis from the unpartitioned GTR+GAMMA model. We visualized the resulting phylogeny and assessed bootstrap support using FigTree v.1.4.2 (Rambaut, 2015).

Maximum parsimony (MP) analyses were conducted using PAUP* 4.0b10 program (Swofford, 2003). All heuristic searches were performed using MULTREES (allowing multiple trees constructions for heuristic searches) with 1,000 replicates, employing the random addition of taxa, retaining only the best tree, holding 10 trees at each step using tree bisection-reconnection (TBR) branch swapping, and collapsing zero-length branches. Bootstrap values were calculated using 1,000 replicates with the following options selected: heuristic search, TBR branch swapping, collapse of zero-length branches, and random-sequence-addition with one replicate.

Pairwise sequence divergence based on K2P distances were calculated using MEGA6 (Tamura et al., 2013) and the proportion of missing data was calculated using Mesquite (Maddison and Maddison, 2017). Net synonymous divergence between species was calculated with MEGA7 (Kumar et al., 2016).

2.5. Population structure and admixture

An admixture analysis was implemented in STRUCTURE v.2.3.1 (Pritchard et al., 2000) using SNP frequency data to better visualize genomic variation between individuals. Ten replicates were run at each value of *K* between 2 and 5 for *E. immersa* group and *K*=9 for *E. longicornis* group. Each run had a burn-in of 10K generations followed by 20K generations of sampling. We used StrAuto to automate Structure processing of samples (Chhatre and Emerson, 2017). Replicates were permuted in the program CLUMPP (Jakobsson and Rosenberg, 2007) according to the ad hoc ΔK statistics (Evanno et al., 2005), which is the second-order rate of change of the likelihood function. Structure results were visualized using the program DISTRUCT (Rosenberg, 2004).

We used four-taxon D-statistics (Durand et al., 2011) for introgression analysis. For the test, 1,000 bootstrap replicates were performed to measure the standard deviation of the D-statistics. Significance was evaluated by converting the Z-score (which represents the number of standard deviations from zero from D-statistics) into two tailed P-values, and using α=0.01 as a conservative cut-off for significance after correcting for multiple comparisons using Holm-Bonferroni correction. All D-statistics were calculated in pyRAD v.3.0.64 (Eaton, 2014). In order to run interactive data analysis, the Python Jupyter notebooks (http://jupyter.org) were used.

2.6. Cross-contamination detection

To detect identical loci between specimens or groups of specimens in ddRAD data, an R (R Core Team, 2017) script requiring a package *ape* (Paradis and Schliep, 2018) was written. The script takes as an input a text file containing alignments of ddRAD loci (output from *ipyrad*). A table is produced for every locus (rows) and specimen (columns) where cells contain a list of specimens that are identical to a specimen indicated in the column (the cell is empty if there are no identical specimens for a particular specimen and locus). Additional columns are added to get information per locus about identical specimens between two groups, the number of specimens, maximum, median and mean divergence. The two groups examined are *longicornis* (including *E. tridentis*, which taxonomically is not a member of the group, but closely related) and *immersa* groups. For both groups and for every locus, specimens are recorded that are identical to any member in the other group while different from specimens in its own group. The second table produced by the script lists the specimens in the dataset, the number of loci, and the normalised number of loci per specimen. Normalised numbers of loci were calculated as half of the maximum number of loci divided by the number of loci of a particular specimen in the dataset. Then the script proceeds to produce bar plots (output as pdf) for every specimen showing percent of loci and normalised percent of loci that are identical to a particular specimen while different from all others. Two additional bar plots were produced for *longicornis* and *immersa* groups to show percent of loci of a particular specimen that are identical to any specimen in the wrong group while different from specimens in its own group. The script and the dataset with 19 413 loci (Supplementary Data S4, S11) are available on Figshare (http://dx.doi.org/10.6084/m9.figshare.7605404).

3. Results

3.1. Detection of divergent loci and cross-contamination

~~in the process of~~ To explore the RAD data an initial RAxML analysis of the dataset was assembled with a clustering threshold of 80% similarity (29 859 loci, 5 945 539 bp; including *E. immersa* group). In this, *E. japonica* did not form a monophyletic group, as one of the specimens was even outside of the *longicornis* group, forming a sister group to *E. tridentis* and the rest of *E. longicornis* group (Supplementary Data S1). Manual examination of loci found in at least one of the *E. japonica* specimens (about 600 000 bp) revealed about 20 loci containing non-homologous regions to other specimens (divergence roughly 5–10 times higher than the average among the other specimens). These have likely resulted from mis-association of paired-end reads (Supplementary Data S2). In one case we also noticed that one of the *E. japonica* specimens was identical to one specimen of *E. immersa* while clearly different from all other specimens, indicating possible cross-contamination (p-distance to other *immersa* group specimens 0.6–3.4%, distance to the *longicornis* group specimens 8.6–11.2%; Supplementary Data S3). Dataset with problematic loci removed (19 413 loci, 3 517 320 bp) yielded a topology identical to the initial tree except for within species relationships (Supplementary Data S4).

Because the phylogenetic position of *E. japonica* specimens did not change when the divergent loci were removed, we aimed to detect possible cross-contamination in the smaller dataset. For this, we identified for every locus pairs of specimens that were identical to each other while different from the rest. In addition, to specifically get an idea about the level of cross-contamination between *immersa* and *longicornis* groups, we identified loci that showed no difference between individuals of different groups, e.g. between *E. japonica* USNM2051678_003 (hereafter as USNM003) and any specimen in *immersa* group.

Clear outlier with regard to cross-contamination between *immersa* and *longicornis* groups was *E. japonica* USNM003, with 26.7% of its loci (out of 1015) identical to one or more specimens in *immersa* group (Fig. 1a). The cross-contamination in USNM003 seems to have been caused by *E. immersa* DEI-GISHym80071 (Fig. 1b) which alone contributed 8.4% of the sequences of USNM003. Two other *immersa* group specimens were both with only one locus (0.1%) identical to USNM003. Four other cases suggested a significant amount of cross-contamination, ranging from 4.4% to 5.6% of loci identical to specimens in the wrong group (Supplementary Data S5). For the other specimens these percentages were less than 2.5%, and in most cases less than 1% (Supplementary Data S5).

The level of cross-contamination within the *immersa* and *longicornis* groups was more difficult to estimate, because of higher degree of relatedness and at least occasional hybridisations between the species cannot be excluded. Nevertheless, for the *longicornis* group, it seems that in most cases the specimens are free of cross-contamination. For most specimens, the proportion of loci identical to a particular specimen belonging to a different species was less than 2.5% (Supplementary Data S5). A clear exception was *E. japonica* USNM2051678_038 (hereafter as USNM038) with 12.3% of its loci identical to *E. minuta* MH10-01 and 5.1% identical to *E. loktini* (Fig. 1c). The other exception was a pair of *E. longicornis* and *E. tridens* specimens that shared 2.9–4.8% of identical loci, but this might be genuine because these species are closely related and the *E. tridens* specimen (TUZ615023) seems to be highly heterozygous compared to other specimens (0.5% of positions are two-fold degenerate; Supplementary Data S6), increasing the chance for sequences to be identified as identical.

For *E. japonica* USNM038, however, the high number of loci identical to *E. loktini* (5.1%) and especially to a particular specimen of *E. minuta* MH10-01 (12.3%) appeared suspicious, as from a morphological perspective, *E. japonica* is not expected to be specifically related to *E. loktini* or *E. minuta*, but is very similar to *E. tridens* and *E. longicornis*. Only one *E. minuta* specimen from Estonia contributed almost all the identical sequences. The other two *E. minuta* specimens from Estonia and Sweden both contributed only one (0.1%) identical locus. To further check the possibility of contamination, we selected two candidate ddRAD loci of USNM038 that we suspected to be contaminated and to see if the results can be replicated using PCR and Sanger sequencing. In both cases, the Sanger sequencing revealed that *E. japonica* specimens were identical to each other and different from all other specimens, confirming the pattern found in the other Sanger sequenced nuclear markers (Supplementary Data S7). For the other sequenced specimens, the Sanger sequencing results were found to be consistent with the ddRAD data (no substitution differences), but in some cases there were indel differences, which can at least partly be explained by length differences of quality trimmed paired-end reads (Supplementary Data S7).

It is more difficult to recognise possible cross-contamination within the *E. immersa* group, because of the small number of specimens and unresolved taxonomy. Nevertheless, based on morphology and ecology, *E. fletcheri* can be reliably separated from the others in the *immersa* group. At least the two European specimens of *E. fletcheri* (from Estonia and Sweden) did not share significant number of identical loci with a particular specimen from the other species (for each of these specimens the contribution was less than 2.2%; Supplementary Data S5). However, the *E. fletcheri* specimen from Canada, which genetically seems to have little in common with the European counterpart, appeared somewhat contaminated because the largest contributor of identical loci and in quite a large amount (3.4%; Supplementary Data S5) was *E. camtschatica* from Sweden. For other cases in the *immersa* group it is difficult to evaluate if it is a genuine signal or cross-contamination. For example, *E. plana* DEI-GISHym15478 had 7.8% of its loci identical to *E. camtschatica* (Supplementary Data S5), but both are from Sweden and could be the same species despite small differences in the saws (ovipositors).

We subsequently analysed *immersa* and *longicornis* groups separately using datasets assembled with clustering threshold of 95% similarity (both, *de novo* and reference assembly), which decreases the chance of introducing highly divergent regions (Tables 3 and 4). Because both *E. japonica* specimens appeared substantially more cross-contaminated than the other specimens, we decided to exclude them from final analyses, but also examined the effects of including one or both of them in different analyses. We excluded also the third apparently most contaminated specimen, *E. tridens* TUZ615037, from the final analyses (5.6% of loci identical to *E. tridentis*, which is not a member of *immersa* or *longicornis* groups), although its inclusion had almost no effect on the results.

Table 3. Summary statistics of ddRAD and mitochondrial COI barcode data sets from *E. longicornis* and *E. immersa* group.

	E. longicornis group			*E. immersa* group		
	ddRAD_dn	ddRAD_ref	mtDNA	ddRAD_dn	ddRAD_ref	mtDNA
Number of taxa	22	22	22	10	10	10
Assembly method	De novo	Reference	–	De novo	Reference	–
Loci	20,871	943	1	9,362	551	1
SNPs	145,512	4,549	129	44,573	1,359	68
PIS	45,463	1,405	47	14,308	332	45
Alignment length (bp)	3,733,285	161,903	1,536	1,714,773	97,793	1,536
Missing (%)	70.1	67.7	7.7	47.6	53.1	32.1
Base frequency (C/G)	0.21590/	0.23849/	0.14303/	0.21581/	0.23943/	0.14031/

	0.21513	0.23731	0.12937	0.21615	0.22707	0.13571
Number of MP trees	1	–	3	1	–	1
MP tree length	156210	–	169	45200	–	71
Consistency index (CI)	0.856	–	0.799	0.881	–	0.972
Retention index (RI)	0.612	–	0.815	0.644	–	0.971

Note: PIS, parsimony informative SNPs; MP, maximum parsimony.

Table 4. Specimens of *Empria* analysed in this study and a summary of the ddRAD data in *de novo* and reference assembly.

Species	Sample ID	Total reads (million)	*de novo* assembly				Reference assembly				
			Clusters at 95%[a]	Mean depth	Retained loci [b]	Recovered loci	Mapped reads	Clusters total	Clusters depth	Reads consensus	Recovered loci in assembly
(a) *Empria longicornis* group											
E. alector	ealec_DEI_GISHym80142	4.78	227253	20.1	59694	13725	28997	8165	14.9	2699	618
E. alector	ealec_TUZ615036	0.34	14426	11.3	4576	2139	2163	422	26.6	133	70
E. alector	ealec_TUZ615121	4.81	146273	31.1	42238	13311	17241	5081	17.6	1782	620
E. alector	ealec_TUZ615220	2.18	39319	51.6	11234	4894	1	1	4.0	1	NA
E. alpina	ealpi_DEI_GISHym80106	4.24	154599	26.2	45944	6777	19941	5475	17.1	2029	430
E. basalis	ebasa_DEI_GISHym14890	0.72	41354	15.4	16358	6920	2166	1245	5.8	437	267
E. basalis	ebasa_OL10_02	1.01	22225	34.5	4675	1628	718	520	2.9	124	62
E. basalis	ebasa_TUZ615083	0.09	9336	8.9	2817	1354	487	284	2.4	72	47
E. basalis	ebasa_TUZ615141	0.86	50972	15.4	18278	8815	3397	1805	5.9	630	362
E. loktini	elokt_TUZ615180	3.73	87639	38.4	29215	3204	9162	2681	13.7	1049	230
E. longicornis	elong_TUZ615022	2.35	26206	74.4	5274	1888	2710	362	6.7	158	77
E. longicornis	elong_TUZ615057	7.94	169150	43.4	60811	12411	27292	5494	34.5	2648	624
E. minuta	eminu_DEI_GISHym21189	0.47	15693	23.2	8430	1701	2245	615	13.9	321	110
E. minuta	eminu_IZBE0350001	0.99	17678	50.7	7576	1712	678	129	37.7	95	63
E. minuta	eminu_MH10_01	2.47	67598	35.0	30890	5477	8133	2266	16.3	1280	366
E. sp. 11	esp11_USNM2051678_040	0.34	10506	23.1	4687	904	542	337	3.1	137	39
E. sp. 14	esp14_MH11_01	1.34	47172	26.7	23470	6544	3217	857	31.0	495	287
E. tridens	etrid_TUZ615023	2.46	88462	27.0	42207	14400	12408	4209	14.0	2184	732
E. tridens	etrid_TUZ615027	2.23	81560	26.5	36613	12705	13373	3713	19.5	1919	645
E. tridens	etrid_TUZ615165	7.32	87708	65.9	29019	10128	7056	2643	10.4	1257	507
E. tridens	etrid_TUZ615624	1.18	25886	42.8	9701	3738	1815	896	8.8	407	169
E. tridentis	etridt_TUZ615182	2.93	71026	34.6	28846	2866	5943	2607	8.9	1308	270
	AVERAGE	**2.49**	**68275**	**33.0**	**23752**	**6238**	**7713**	**2264**	**14.3**	**962**	**314**
(b) *Empria immersa* group											
E. camtschatica	ecamt_DEI_GISHym80070	1.22	48116	24.2	17103	6835	3061	1591	4.9	562	311
E. fletcheri	eflet_BIOUG17274_F06	11.77	162626	68.7	26945	3803	3008	1474	9.1	415	227
E. fletcheri	eflet_DEI_GISHym31039	0.51	30181	14.6	10985	4306	2333	1131	8.0	398	215
E. fletcheri	eflet_TUZ615334	0.27	28908	9.2	9900	3805	1735	1083	4.2	306	187
E. immersa	eimme_DEI_GISHym80045	0.98	53371	17.1	20648	7866	4804	2265	14.3	823	429
E. immersa	eimme_DEI_GISHym80071	4.09	124234	30.7	41156	8318	13554	4017	21.5	1697	470
E. immersa	eimme_TUZ615623	2.96	79575	34.0	33109	8058	8117	2695	22.8	1231	453

E. improba	eimpr_BIOUG00998_D06	0.39	12918	27.2	4762	1414	668	379	3.2	146	69
E. plana	eplan_DEI_GISHym15478	1.84	24812	29.4	9043	2594	1374	488	8.6	268	110
E. plana	eplan_TUZ615181	0.58	20249	26.3	8695	2109	2226	599	10.1	275	93
	AVERAGE	**2.46**	**58499**	**28.1**	**18235**	**4911**	**4088**	**1572**	**10.7**	**612**	**256**

[a]Clusters that passed filtering for 6x minimum coverage.
[b]Loci retained after passing coverage and paralog filters.
NA, not applicable.

3.2. Empria longicornis group

All species with more than one individual sampled were found to be monophyletic and in most cases strongly supported in maximum likelihood trees reconstructed from ddRAD datasets based on *de novo* and reference assemblies (Figs 2a and 3a). Monophyly of only *E. tridens* was moderately supported based on reference assembly (Fig. 3a). There were some differences in tree topology above the species level based on reference and *de novo* assembly (phylogenetic positions of *E. sp11* and *E. loktini*), but these differences were poorly supported, particularly in the smaller dataset based on the reference assembly (Figs 2a and 3a).

Monophyly of most species defined based on morphology was also well supported by concatenated analysis of three nuclear protein coding genes obtained by Sanger sequencing (Fig. 4d). Of the species for which more than one individual was sampled, only *E. tridens* was not monophyletic according to the three-gene tree. The species for which only one individual was sampled (*E. alpina*, *E. loktini*, sp11) were well separated from the other species as well as from each other based both on ddRAD and Sanger data, supporting their species status (Figs 2a, 3a, 4d). For *E. montana* Koch, 1984 we were not able to obtain enough ddRAD data to be included in the analyses (Supplementary Data S8), but based on Sanger sequencing of three specimens, we can confirm that it belongs to the *longicornis* group (Supplementary Data S9 and S10). *Empria montana* was not recognised by Prous et al. (2011b) as a member of *longicornis* group because of divergent penis valve (only holotype male was known at the time). Two of the studied specimens of *E. montana* (http://dx.doi.org/10.6084/m9.figshare.7447847; http://dx.doi.org/10.6084/m9.figshare.7447874) were reared from *Dasiphora fruticosa*, which was previously unknown. Based on current genetic sampling of three *E. montana* specimens (two from Magadan oblast, one from Krasnoyarsk Krai, Russia), this species is monophyletic according to mitochondrial COI (Supplementary Data S10). Partial fragments of three nuclear genes used here are available for only one *E. montana* specimen, based on which this species groups together with *E. alpina*, *E. minuta*, and sp11, but in an unresolved position (Supplementary Data S9).

Distance calculations of ddRAD data (*de novo* assembly) were also consistent with species limits defined based on morphology (Table 5). Mean within species divergence varied between 0.18–0.92%, while distances among species were about twice as high, 1.05–1.87%.

Table 5. Mean pairwise distances of ddRAD (below diagonal) and mtDNA data (above diagonal) within (grey shaded cells; ddRAD de novo assembly data/mtDNA) and between the species.

(a) *E. longicornis* group and *E. tridentis*

	alec	alpi	basa	lokt	long	minu	sp11	sp14	trid	tridt
alecor	0.35/1.20	0.74	1.54	1.82	1.00	1.07	1.82	1.80	1.36	5.07
alpina	1.78	NA	1.58	1.76	0.79	0.59	1.76	1.67	1.21	5.01
basalis	1.08	1.70	0.50/1.01	1.58	0.93	1.51	1.90	1.90	0.94	5.26
loktini	1.87	1.83	1.77	NA	1.53	1.50	0	1.95	1.66	4.56
longicornis	1.24	1.77	1.13	1.80	0.18/1.24	0.99	1.53	1.63	0.74	5.05
minuta	1.73	1.70	1.61	1.85	1.69	0.52/0.79	1.50	1.49	1.33	4.87
sp.11	1.82	1.60	1.72	1.73	1.87	1.69	NA	1.95	1.66	4.56
sp.14	1.55	1.60	1.53	1.84	1.52	1.75	1.79	NA	1.86	5.34
tridens	1.17	1.73	1.05	1.84	1.09	1.74	1.84	1.52	0.92/0.97	5.23
tridentis	2.08	2.07	1.99	1.99	2.10	2.10	2.02	2.08	2.01	NA

(b) *E. immersa* group

	camt	flet	imme	impr	plan
camtschatica	NA	2.30	1.90	2.74	1.42

fletcheri	1.14	0.94/2.88	1.99	2.24	2.39
immersa	0.88	1.34	0.49/1.21	2.68	2.47
improba	1.18	1.31	1.42	NA	3.72
plana	1.02	1.31	1.22	1.17	1.15/2.02

NA, not applicable because of single specimen.

Based on nuclear NaK, POL2, and ZC3H14 (altogether 5646 bp), net synonymous divergences among most of the species (7 species for which more than one individual was sampled) were between 2.3–9.4%, suggesting that these species are well separated (Roux et al., 2016). Divergence between only *E. basalis* and *E. tridens* (1.5%) fell within the grey zone of speciation according to Roux et al. (2016).

Phylogenies based on ddRAD and combined data of three nuclear protein coding genes (NaK, POL2, and ZC3H14) were largely congruent when considering well supported relationships (bootstrap support more than 70%). Moderately supported differences involved relationships among *E. minuta*, *E. alpina*, and sp11, which formed a clade based on the three-gene dataset (Fig. 4d), but not based on ddRAD data (Figs 2a and 3a). There were some strongly or moderately supported phylogenetic differences among the three protein coding genes. According to the gene tree of POL2 (Fig. 4b), *E. longicornis* and *E. japonica* formed a strongly supported clade, which was absent in the other two gene trees (NaK and ZC3H14) (Figs 4a and 4c). The second, moderately supported difference was non-monophyly of sp14 according to ZC3H14 (Fig. 4c), contrary to POL2 (Fig. 4b) (according to NaK it was unresolved). Another, moderately supported difference was between NaK and ZC3H14 on one hand and POL2 on the other. According to NaK and ZC3H14 (Figs 4a and 4c), *E. alpina*, *E. minuta*, and sp11 formed a clade (although relationships among these three species differed, but without strong support), but *E. minuta* was weakly supported as basal to all other *longicornis* group species in POL2 tree (Fig. 4b). These differences between single genes can be expected in closely related species complexes because of incomplete lineage sorting, which can cause incompatibilities between gene and species trees even without hybridisation.

Admixture analysis with STRUCTURE at K=9 (the number of species based on morphology, excluding *E. japonica*) supported most species as largely separate populations from each other (Fig. 2a). Best supported were *E. alector*, *E. basalis*, *E. longicornis*, *E. minuta* and sp11, which appeared to have very little or no contribution from other species (Fig. 2a). Reasonably well supported were *E. loktini* and sp14, while *E. tridens* and *E. alpina* apparently had significant contributions from some other species (Fig. 2a). However, there were inconsistencies among different STRUCTURE analyses. When both *E. japonica* specimens were included (at K=10), *E. alpina* was better supported, while *E. longicornis* received less support, as it seemed to have a large contribution from *E. basalis* (Supplementary Data S11).

The results of four-taxon D-statistic tests suggested numerous cases of introgression between different species. The most strongly supported case involved *E. minuta* and sp14 (Table 6), but curiously this received (almost) no support from STRUCTURE analyses (Fig. 2a, Supplementary Data S11). In contrast to STRUCTURE (Fig. 2a) and D-statistic tests (Table 6), the counting of the number of identical loci between the specimens suggested the largest contributor to be *E. alpina* (1.5%) in case of sp14 (*E. minuta* contributed 0.5%, Supplementary Data S5), which found some support in the STRUCTURE analysis when both *E. japonica* specimens were included (Supplementary Data S11). There were numerous other inconsistencies among the four-taxon D-statistic tests, different STRUCTURE analyses and the counting of identical loci.

Table 6. Four-taxon D-statistic tests results showing significant replicates for introgression in *Empria*.

Test	P1[1]	P2	P3	O	Range Z[2]	nSig/n[3]	nSig/n (%)[4]
(a) *E. longicornis* group (28 cases out of 44)							
a1	T	T	L	Tt	0.1 – **15.9**	5/11	45.5
a2	T	T	B	Tt	0.3 – **15.4**	7/23	30.4
a3	T	T	Ac	Tt	0.0 – **10.2**	4/17	23.5
a4	T	T	Sp14	Tt	0.1 – **17.5**	2/5	40.0
a5	T	T	Sp11	Tt	0.3 – **9.4**	2/5	40.0
a6	T	T	M	Tt	0.0 – **20.8**	6/17	35.3
a7	T	T	Ap	Tt	0.0 – **6.9**	1/5	20.0
a8	T	T	Lt	Tt	0.1 – **5.6**	2/5	40.0
a9	L	L	B	Tt	1.5 – **3.3**	1/3	33.3
a10	L	L	M	Tt	0.5 – **18.8**	1/3	33.3
a11	B	B	T	Tt	0.0 – **13.6**	2/23	8.7
a12	B	B	L	Tt	0.0 – **3.5**	1/11	9.1
a13	B	B	Ac	Tt	0.0 – **8.2**	3/17	17.6
a14	B	B	sp14	Tt	0.2 – **13.3**	3/5	60.0
a15	B	B	sp11	Tt	0.0 – **3.5**	1/5	20.0
a16	B	B	M	Tt	0.5 – **6.4**	1/5	20.0
a17	B	B	Lt	Tt	0.0 – **10.2**	4/17	23.5
a18	Ac	Ac	B	Tt	0.0 – **4.6**	1/11	9.1
a19	M	M	T	Tt	0.0 – **17.2**	2/11	18.2
a20	M	M	L	Tt	0.2 – **3.8**	1/5	20.0
a21	M	M	B	Tt	0.1 – **12.3**	3/11	27.3
a22	M	M	Ac	Tt	0.0 – **3.9**	2/8	25.0
a23	M	M	Sp14	Tt	17.8 – **38.5**	3/3	100.0
a24	M	M	Sp11	Tt	0.0 – **10.0**	1/3	33.3
a25	(T+L)	(T+L)	B	Tt	0.0 – **15.3**	26/59	44.1
a26	B	B	(T+L)	Tt	0.0 – **13.5**	2/35	5.7
a27	(T+L+B)	(T+L+B)	Ac	Tt	0.0 – **13.7**	23/134	17.2
a28	Ac	Ac	(T+L+B)	Tt	0.0 – **4.7**	1/29	3.4
(b) *E. immersa* group (7 cases out of 26)							
b1	F	F	C	Im	0.0 – **3.5**	1/3	33.3
b2	Im	Im	F	Ip	0.4 – **8.8**	1/8	12.5
b3	Im	Im	Ip	F	0.0 – **3.5**	1/5	20.0
b4	(F+Ip)	(F+Ip)	(C+P)	Im	0.0 – **3.8**	1/19	5.3
b5	(C+P)	(C+P)	(F+Ip)	Im	2.3 – **5.4**	3/4	75.0
b6	(F+Ip)	(F+Ip)	Im	P	0.0 – **6.0**	6/29	20.7
b7	(F+Ip)	(F+Ip)	Im	C	0.0 – **6.7**	3/29	10.3

[1]Taxon names are abbreviated: In *E. longicornis* group, Ac: *E. alector*, Ap: *E. alpina*, B: *E. basalis*, L: *E. longicornis*, Lt: *E. loktini*, M: *E. minuta*, Sp11: *Empria* sp.11, Sp14: *Empria* sp.14, T: *E. triden*, Tt: *E. tridentis*. In *E. immersa* group, C: *E. camtschatica*, F: *E. fletcheri*, Im: *E. immersa*, Ip: *E. improba*, P: *E. plana*. Tests are referred to by number in the text. Insignificant cases are not shown.

[2]Bold indicates significance at α=0.01.

[3]Significant tests over possible sampled individuals.

[4]The percentage was calculated for the number of significant replicates shown (nSig) out of all possible four-sample replicates (n) in each test.

In contrast to nuclear data, mitochondrial COI did not support monophyly of any species (except possibly *E. montana* and sp14: Supplementary Data S10) and in some cases the non-monophyly was strongly supported (Fig. 2a). Besides the non-monophyly of species, the general topology of COI tree was very different from nuclear ML tree (Fig. 2a).

3.3. Empria immersa group

Morphologically defined species boundaries in the *immersa* group (Prous et al., 2014) are not as well supported as in the *longicornis* group. Only *E. immersa* based on ddRAD data and combined analyses of NaK and POL2 genes (but not in analysis based only on POL2), and *E. improba* based on limited amount of ddRAD data were found to be monophyletic (Figs 2b, 3b, Supplementary Data S12). Although two or three (depending on the dataset) specimens of European *E. fletcheri* (from Scotland, Sweden, and Estonia) unambiguously grouped together in all analyses (Figs 2b, 3b, Supplementary Data S12), they did not appear to be closely related to the single analysed North-American counterpart (Figs 2b, 3b). Within and between species divergences based on ddRAD data (*de novo* assembly) in the *immersa* group partly overlapped. Within species divergences (0.49–1.15%) were somewhat larger compared to the *E. longicornis* group, while between species divergences were somewhat smaller (0.88–1.42%) (Table 5).

Similarly to the *longicornis* group, there were some differences between NaK and POL2 phylogenies, one of which was rather well supported. *Empria immersa* was moderately supported as monophyletic according to NaK (Fig. 4a), but not according to POL2 (Fig. 4b), in which case two specimens of *E. immersa* were not separated from *E. camtschatica*, *E. improba*, and *E. plana*. Based on these two genes (altogether 4061 bp), net synonymous divergences between three species for which more than one individual was sampled were between 1.0–2.0%, therefore falling within the grey zone of speciation according to Roux et al. (2016). When only *E. immersa* and European *E. fletcheri* were considered (because North-American *E. fletcheri* did not group with European ones and *E. plana* was not monophyletic), net synonymous divergence between these species was 2.9%, falling outside the grey zone (Roux et al., 2016).

Admixture analysis with STRUCTURE at *K*=5 (the number of species based on morphology) did not support the current taxonomy very well either, as only *E. immersa* and the European specimens of *E. fletcheri* were consistently supported as distinct populations from the others (Fig. 2b, Supplementary Data S11). Curiously, *E. camtschatica* and *E. improba* were supported as part of almost the same population, even though they were far apart in the ddRAD tree (Fig. 2a). Morphologically these two species could be the same, but STRUCTURE analyses with a different taxon sampling suggested that *E. camtschatica* and *E. improba* are largely separate populations (Supplementary Data S11). Interestingly, at *K*=3, STRUCTURE suggested that there are three clearly separated populations: European *E. fletcheri*, *E. immersa*, and the other species together (Fig. 5, Supplementary Data S11). North-American *E. fletcheri* was a mixture of *E. camtschatica*, *E. improba, E. plana,* and European *E. fletcheri* according to STRUCTURE analyses at *K*=2 to *K*=5 (Fig. 5).

The results of four-taxon D-statistic tests suggested some cases of possible introgression between different species (Table 6).

As in the *longicornis* group, nuclear and mitochondrial trees of the *immersa* group were very different from each other and monophyly of species was not supported (Fig. 2b).

4. Discussion

4.1. Cross-contamination or hybridisation?

The large amount of data generated with high-throughput sequencing methods precludes manual checking of every alignment. The main problems with these datasets are the introduction of non-homologous alignment regions and contaminations, which would be easy to notice when dealing only with few genes by checking every alignment and gene tree. Because the species in our dataset are all closely related, the exclusion of non-homologous alignments is relatively easy by increasing clustering similarity threshold (up to 90% or 95% in our case) together with use of stringent filtering steps, which excludes all or most problematic alignments. However, in studies that pool specimens for sequencing and use single barcode or barcode combinations (but fewer unique barcodes than specimens) to link the reads to specimens after sequencing, it becomes especially difficult to detect cross-contamination when study organisms are closely related, because it might not be obvious if identical loci between specimens are due to biological or technical reasons. Nevertheless, the two species-groups of *Empria* studied here are morphologically and genetically (based on both mitochondrial and nuclear DNA) well separated (Prous, 2012) and hybridisations between them are unlikely. Therefore, by examining patterns of identical loci between the groups, it is possible to get an estimation of the level of cross-contamination in our dataset.

In the dataset excluding divergent loci (19 413 loci, Supplementary Data S11), about 6% of the sequences involve identical pairs between *immersa* and *longicornis* groups (in order not to exclude any specimens, *E. tridentis* was treated as a member of the *longicornis* group in these pairwise comparisons). This percentage is certainly an over-estimation regarding cross-contamination as many of the loci (which are short, about 180 bp) might be too conserved to reveal differences between the groups. Better indication would be examination of the cases where one specimen is identical to any other in the wrong group while different from specimens in its own group (if present). In this case 1% of all sequences are identical to specimen(s) in the wrong group. Assuming the same cross-contamination rate within *immersa* and *longicornis* groups themselves suggests 2.4% of the sequences of the whole dataset to be affected (58% of pairwise comparisons are within *immersa* and *longicornis* groups). It is difficult to say if this is still over-estimation or instead under-estimation. Based on a more stringent criterion, e.g. considering loci present for four or more specimens from both groups (i.e. at least 8 specimens) gives a cross-contamination rate of 0.6% for the whole dataset. Studies that specifically examined cross-contamination have found that barcode jumps can cause 0.3–2.5% of the sequence reads to be assigned to a wrong individual (Kircher et al., 2012; Schnell et al., 2015). A cross-contamination level of 1–2% could be considered acceptable if it affected every specimen equally, but might still lead to questionable conclusions if some specimens were affected much more than others (van der Valk et al., 2019).

In our dataset two *E. japonica* specimens were outliers regarding possible cross-contamination (Fig. 1). Besides the fact that the largest number of identical loci in both cases was contributed by a species different from *E. japonica* (which in one case even belonged to a different species group), two additional arguments support the cross-contamination explanation over hybridisation. Firstly, the individuals contributing the largest number of identical loci in *E. japonica* specimens belong to *E. immersa* (from Sweden, Fig. 1b) or *E. minuta* (from Estonia, Fig. 1c). At the same time, the other specimens of *E. immersa* (from Sweden and Finland) and *E. minuta* (Estonia and Sweden) did not contribute almost any identical loci (one or two) to the *E. japonica* specimens. It is highly unlikely

that specimens of *E. immersa* and *E. minuta* from Sweden and Estonia share genes almost exclusively with one or the other specimen of *E. japonica* from Hokkaido (Japan) because of introgression, while this is not seen between other specimens of the same species. If introgression was the likely cause in these cases, one would expect to see comparable levels of gene sharing in other specimens and preferably between specimens in geographic proximity (most studied specimens are from Europe). Secondly, PCR and Sanger sequencing of two loci that were suspected to be cross-contamination in one of the *E. japonica* specimens contradicted the ddRAD data: sequences of two or three *E. japonica* specimens were identical to each other while different from all the other sequenced specimens (Supplementary Data S7). Although our dataset overall might not be affected by a higher level of cross-contamination than usual (e.g. Schnell et al., 2015), the relatively high level of unequal recovery of loci (difference more than 10 times) among the specimens might explain why some of them were affected proportionally more than others (van der Valk et al., 2019). Among the specimens retained for the analyses, both *E. japonica* specimens were at the lower end of the number of loci recovered. If more loci had been recovered from both *E. japonica* specimens, these might have diluted the cross-contamination and we might not have realised that possibility. It is likely that some (perhaps even most) other specimens in our dataset have also been affected by cross-contamination (including among conspecific individuals which we could not detect) to some degree, weakening our biological conclusions for the studied species groups. Nevertheless, except in the case of *E. japonica*, the results based on ddRAD data seem plausible in the light of morphological studies (Prous, 2012; Prous et al., 2014, 2011b) and Sanger sequencing (Fig. 4), but should be re-examined in future studies with better control for cross-contamination. Although more expensive, we suggest that whenever possible, additional replications should be done with different combinations of pooled specimens, pooling only distantly related species, sequencing every specimen separately, or adding specimen specific barcodes to both ends of the DNA fragments (not just different combinations of limited number of barcodes).

Even if 1–2% is considered an acceptable level of erroneous sequences (because of non-homology and/or contaminations) in phylogenomic datasets, their effect in downstream analyses can remain significant. It is likely that even a small proportion of errors could be detrimental to reconstructing rapid speciation events if the small amount of signal is swamped by a larger amount of error. On the other hand, resolving rapid speciation events would be among the questions to which large datasets could give the largest contribution (uncontroversial clades can be reliably reconstructed already based on small number of genes) and therefore data quality is essential before deciding among alternative phylogenetic hypotheses. Unfortunately, the bioinformatic tools are not yet reliable enough to completely remove the necessity of manual interventions in phylogenomic datasets (Philippe et al., 2017; Simion et al., 2017).

4.2. Causes of mitonuclear discordance

In both studied species groups, mitochondrial phylogeny is very different from nuclear phylogeny (Fig. 2). Particularly striking is the non-monophyly of all or most species according to mitochondrial DNA, while there is little incongruence between nuclear and morphological evidence (Figs 2–4; Prous, 2012; Prous et al., 2011b). Strong mitonuclear discordance has been observed in other animal groups and usually interpreted as evidence of mitochondrial introgression (e.g. Bronstein et al., 2016; Papakostas et al., 2016; Tang et al., 2012), which does seem to be the most likely explanation (Bonnet et al., 2017; Sloan et al., 2017), although it may also result from incomplete lineage sorting (Funk and Omland, 2003). Recently, Patten et al. (2015) found based on theoretical modelling that haplodiploid species may be especially prone to biased mitochondrial introgression, which could explain widespread mitonuclear discordance in several other species rich sawfly groups even when taxonomic oversplitting has been taken into account, like *Neodiprion*

(Linnen and Farrell, 2008, 2007) and *Pristiphora* (Prous et al., 2017). Nevertheless, haplodiploidy is probably not the only factor promoting widespread mitonuclear discordance, because in many other (most?) Hymenoptera, mitochondrial barcoding seems to work relatively well for species identification (Derocles et al., 2012; Klopfstein, 2014; Schmidt et al., 2015). Another factor that might influence rate of mitochondrial introgression is its mutation rate, lower rates making introgression more probable than higher rates, latter of which should more likely lead to compensatory co-evolution and mitonuclear incompatibilities (see Table 3 in Sloan et al., 2017). As mitochondrial genomes of basal hymenopterans do evolve significantly more slowly than in Apocrita (particularly Xyeloidea, Pamphilioidea, and Tenthredinoidea; Niu et al., 2019; Tang et al., 2019), the combination of haplodiploidy and slow rate of mitochondrial evolution might better explain widespread mitonuclear discordance in some (many?) species rich groups of sawflies rather than just haplodiploidy. There is evidence that in parasitic lineages mitochondrial evolution tends to be much faster than non-parasitic lineages (Pentinsaari et al., 2016), explaining perhaps faster evolution of mtDNA in Apocrita which are ancestrally parasitic (and most species still are). It could be then that in most Hymenoptera (Apocrita), COI barcoding might be reliable for species identification despite ~~of~~ haplodiploidy.

4.3. Taxonomy of E. longicornis group

Since the revision of the species group (Prous et al., 2011b), two additional putative species have been found, and a third already described species (*E. montana*) is here for the first time recognised as member of the *longicornis* group (Supplementary Data S9 and S10), bringing the total number of species to 12. The male specimen USNM2051678_040 from Hokkaido is so far the only known representative of a putative species "sp11" (sp.1 in Prous et al., 2011a). Because there has been very little sampling of sawflies in arctic habitats above the treeline in Japan (and more generally outside Europe), ~~the~~ sp11 might normally be restricted to arctic habitats like *E. alpina* (sister species of sp11 according to some ddRAD trees: Fig. 2), although the single known specimen was collected in a Malaise trap well below the treeline (at 1000 m, about 15 km East of Mount Asahi, the highest point on Hokkaido). We have studied several specimens of the second putative species, sp14 (male MH11-01 and female DEI-GISHym15231 reported here) collected in the Pyrenees and the Alps, in most cases below the treeline, but at higher altitudes than 1500 m. Morphologically, the only rather clear indication that sp14 might be a different species from *E. alpina* is the different structure of female ovipositor. Male penis valves do not seem to be different in *E. alpina* and sp14, but there is variation in the length of antennae. Confusingly, though, *E. alpina* in the Alps have distinctly longer antenna (both male and female) than the specimens from northern Fennoscandia, the latter of which have antenna more similar to sp14 in the Alps. Although several additional female and possibly male specimens of sp14 are available, we refrain from describing a new species, because more studies are required to ~~more~~ reliably resolve the taxonomy of *E. alpina* and sp14, and to associate males and females. Prous et al. (2011b) noted that there might be an additional species amongst *E. tridens*, based on differences in larval colour pattern and diverging ITS sequences, but the data was too limited to decide this (no differences in adult morphology were detected). One of the specimens analysed here is the larva with diverging ITS sequence and a different colour pattern (TUZ615027, 06-05a in Prous et al., 2011b), but our ddRAD data and Sanger sequenced genes (Figs 2–4) do not clearly indicate that it should be treated as a different species. When excluding *E. alpina*, for which we lack a sufficient amount of fresh material, *E. tridens* is known to be geographically the most widely distributed (from Europe to Hokkaido) among the remaining species (Prous et al., 2011a), which might explain the higher genetic diversity of this taxon, rather than indicating presence of an additional species. For other species with more than one individual sampled (*E. alector, E. basalis, E. longicornis, E. minuta*) our results (Figs 2–4) agree perfectly with current taxonomy (Prous et al., 2011b) and do not suggest the presences of additional species. For *E. japonica*, Sanger data

unambiguously supports validity of this species (Fig. 4) and it is found to be monophyletic also based on ddRAD data when the *immersa* group (which might be source of cross-contamination in one *E. japonica* specimen) is excluded (Supplementary Data S12). Validity of the species is also supported by net synonymous divergences among species based on three protein coding genes (NaK, POL2, and ZC3H14), which in most cases (2.3–9.4%) fall outside the grey zone of speciation according to Roux et al. (2016). Only lesser divergence (1.5%) falling within the grey zone exists between *E. basalis* and *E. tridens* (according to Roux et al., 2016 the grey zone of speciation falls within 0.5%–2.0% of net synonymous divergence between species). A limitation of our dataset regarding species delimitation could be the lack of sampling of specimens of the same species from a wider area than Europe, although at least some of them are known from West or Central Europe to East Asia (Prous et al., 2011b; Taeger et al., 2018). *Empria alector, E. basalis, E. longicornis,* and *E. minuta* were well supported as monophyletic (Figs 2–4), but this needs to be tested by sampling additional specimens from West and East Siberia.

4.4. Taxonomy of E. immersa group

Based on adult morphology there should be at least two species within the *E. immersa* group: *E. fletcheri* (feeding on *Betula*) and the others (feeding on *Salix*). The saw (ovipositor) of *E. fletcheri* is clearly different from *Salix* feeding species. There is quite a clear difference also in the structure of tarsal claws: *E. fletcheri* has a small subapical tooth, while in the others it is distinctly longer (except in one possibly additional species not sampled here: *E. asiatica* that has a saw indistinguishable from *E. camtschatica* and *E. improba*). All of the *Salix* feeding species are very similar in adult morphology and may perhaps belong to same species. However, among the *Salix* feeders, genetic data suggests separation of *E. immersa* from the others (Figs 2–5), which might be supported by differences in colouration of larvae (based on unpublished *ex-ovo* rearings of *E. immersa* and *E. camtschatica*) and some morphological differences in the adults (Prous et al., 2014). Admixture analysis with Structure at K=3 (Fig. 5) suggests that *Empria camtschatica*, *E. plana*, and *E. improba* might belong together, which does not seem unlikely based on morphology (in this case the species name to be applied would be *E. improba* (Cresson, 1880), as the oldest), although more sampling throughout Asia and North-America for genetic studies would be preferable before deciding among competing scenarios. Another issue requiring more attention is the apparently clear genetic separation of European and North-American *E. fletcheri*, which from a morphological perspective clearly belong together. Considering that habitats of *E. fletcheri* (bogs in boreal forests and tundra) in Eurasia and North-America were at least partly connected about 10 000 years ago, this species might well be Holarctic in distribution (in Eurasia the eastern-most specimens confirmed so far are from Irkutsk region). Unfortunately, our data does not currently allow disentangling effects of wide geographic separation and biological barriers to gene-flow in *immersa* and *longicornis* groups. In the ~~case of~~ *longicornis* group, where taxonomy of most species is better resolved than in the *immersa* group, none of the species analysed here include individuals collected outside Europe, although at least some of the species reach East Asia (Prous et al., 2011b; Taeger et al., 2018). Because species within the *longicornis* and *immersa* groups are closely related (within and between-species genetic distances are quite similar, Table 5) conspecific samples analysed from a much larger area than Europe might significantly complicate species delimitation based on genetic data. To test this, additional samples from Central and Eastern parts of Asia should be analysed. In ~~case of~~ *E. fletcheri*, detection of two distinct genetic lineages living in sympatry in East-Asia or North-America would be a strong indication for additional species, but our data is currently insufficient to decide this (for example *E. plana* from Sweden and Hokkaido are also genetically far apart: Figs 2–4).

5. Conclusions

The studied *Empria longicornis* and *immersa* groups have been a taxonomic challenge and previous results based on a limited amount of genetic data suggested widespread mitonuclear discordance and barcode sharing between closely related species. Overall, the phylogenomic data obtained here supports the previous delineation of species and confirms widespread mitonuclear discordance probably resulting from introgression of slowly evolving mitochondrial DNA. A notable exception was non-monophyly of *E. japonica* based on ddRAD data (but not based on Sanger sequencing of three nuclear genes), most likely resulting from cross-contamination due to molecular tag jumps used to identify sequencing reads. Because tag jumps affecting 1–2% of sequencing reads do~~es~~ not seem to be unusual, we recommend considering such possible confounding effects more carefully. Our R script for analysing ddRAD can be used to check if ~~there are~~ specimens share an unexpected number of identical loci. Additional ddRAD sequencing with different combinations of pooled specimens, sequencing every specimen separately, or adding specimen-specific barcodes to both ends of the DNA fragments (not just different combinations of a limited number of barcodes) could be used to minimise possibilities for cross-contamination.

Acknowledgements

We thank Laura Törmälä for her efficient work in the biology laboratory at University of Oulu. We also wish to acknowledge CSC – IT Centre for Science, Finland for computational resources. Matthias Hoffman (ZALF, Müncheberg) and Riina Klais (Tartu) helped with an R script. Andrew Liston (SDEI, Müncheberg) kindly checked the English. Funding: This work was supported by Finnish Academy grant #277984 to MM. MP was supported by the Swedish Taxonomy Initiative. KML acknowledges financial support from the Kvantum Institute.

Competing interests statement

The authors have no competing interests to declare.

Appendix A. Supplementary material

Supplementary data to this article can be found online at https://doi.org/10.1016/…

References

Alex Smith, M., Fernández-Triana, J.L., Eveleigh, E., Gómez, J., Guclu, C., Hallwachs, W., Hebert, P.D.N., Hrcek, J., Huber, J.T., Janzen, D., Mason, P.G., Miller, S., Quicke, D.L.J., Rodriguez, J.J., Rougerie, R., Shaw, M.R., Várkonyi, G., Ward, D.F., Whitfield, J.B., Zaldívar-Riverón, A., 2013. DNA barcoding and the taxonomy of Microgastrinae wasps (Hymenoptera, Braconidae): impacts after 8 years and nearly 20 000 sequences. Mol. Ecol. Resour. 13, 168–176. https://doi.org/10.1111/1755-0998.12038

Bonnet, T., Leblois, R., Rousset, F., Crochet, P.A., 2017. A reassessment of explanations for discordant introgressions of mitochondrial and nuclear genomes. Evolution (N. Y). 71, 2140–2158. https://doi.org/10.1111/evo.13296

Bronstein, O., Kroh, A., Haring, E., 2016. Do genes lie? Mitochondrial capture masks the Red Sea collector urchin's true identity (Echinodermata: Echinoidea: Tripneustes). Mol. Phylogenet. Evol. 104, 1–13. https://doi.org/10.1016/j.ympev.2016.07.028

Chhatre, V.E., Emerson, K.J., 2017. StrAuto: automation and parallelization of STRUCTURE analysis. BMC Bioinformatics 18, 192. https://doi.org/10.1186/s12859-017-1593-0

Cruaud, P., Rasplus, J.-Y., Rodriguez, L.J., Cruaud, A., 2017. High-throughput sequencing of

multiple amplicons for barcoding and integrative taxonomy. Sci. Rep. 7, 41948. https://doi.org/10.1038/srep41948

Derocles, S. a P., LE Ralec, A., Plantegenest, M., Chaubet, B., Cruaud, C., Cruaud, A., Rasplus, J.-Y., 2012. Identification of molecular markers for DNA barcoding in the Aphidiinae (Hym. Braconidae). Mol. Ecol. Resour. 12, 197–208. https://doi.org/10.1111/j.1755-0998.2011.03083.x

Durand, E.Y., Patterson, N., Reich, D., Slatkin, M., 2011. Testing for Ancient Admixture between Closely Related Populations. Mol. Biol. Evol. 28, 2239–2252. https://doi.org/10.1093/molbev/msr048

Eaton, D.A.R., 2014. PyRAD: assembly of de novo RADseq loci for phylogenetic analyses. Bioinformatics 30, 1844–1849. https://doi.org/10.1093/bioinformatics/btu121

Eaton, D.A.R., Overcast, I., 2016. ipyrad: interactive assembly and analysis of RADseq data sets. Available from: http://ipyrad.readthedocs.io/ [WWW Document].

Evanno, G., Regnaut, S., Goudet, J., 2005. Detecting the number of clusters of individuals using the software structure: a simulation study. Mol. Ecol. 14, 2611–2620. https://doi.org/10.1111/j.1365-294X.2005.02553.x

Funk, D.J., Omland, K.E., 2003. Species-Level Paraphyly and Polyphyly: Frequency, Causes, and Consequences, with Insights from Animal Mitochondrial DNA. Annu. Rev. Ecol. Evol. Syst. 34, 397–423. https://doi.org/10.1146/annurev.ecolsys.34.011802.132421

Hebert, P.D.N., Braukmann, T.W.A., Prosser, S.W.J., Ratnasingham, S., DeWaard, J.R., Ivanova, N. V., Janzen, D.H., Hallwachs, W., Naik, S., Sones, J.E., Zakharov, E. V., 2018. A Sequel to Sanger: amplicon sequencing that scales. BMC Genomics 19, 219. https://doi.org/10.1186/s12864-018-4611-3

Hebert, P.D.N., Cywinska, A., Ball, S.L., DeWaard, J.R., 2003. Biological identifications through DNA barcodes. Proc. R. Soc. London. Ser. B Biol. Sci. 270, 313–321. https://doi.org/10.1098/rspb.2002.2218

Hebert, P.D.N., Ratnasingham, S., Zakharov, E. V, Telfer, A.C., Levesque-Beaudin, V., Milton, M.A., Pedersen, S., Jannetta, P., DeWaard, J.R., 2016. Counting animal species with DNA barcodes: Canadian insects. Philos. Trans. R. Soc. B Biol. Sci. 371, 20150333. https://doi.org/10.1098/rstb.2015.0333

Ivanov, V., Lee, K.M., Mutanen, M., 2018. Mitonuclear discordance in wolf spiders: Genomic evidence for species integrity and introgression. Mol. Ecol. 27, 1681–1695. https://doi.org/10.1111/mec.14564

Jakobsson, M., Rosenberg, N.A., 2007. CLUMPP: a cluster matching and permutation program for dealing with label switching and multimodality in analysis of population structure. Bioinformatics 23, 1801–1806. https://doi.org/10.1093/bioinformatics/btm233

Kaltenpoth, M., Showers Corneli, P., Dunn, D.M., Weiss, R.B., Strohm, E., Seger, J., 2012. Accelerated evolution of mitochondrial but not nuclear genomes of hymenoptera: new evidence from crabronid wasps. PLoS One 7, e32826. https://doi.org/10.1371/journal.pone.0032826

Kircher, M., Sawyer, S., Meyer, M., 2012. Double indexing overcomes inaccuracies in multiplex sequencing on the Illumina platform. Nucleic Acids Res. 40, 1–8. https://doi.org/10.1093/nar/gkr771

Klopfstein, S., 2014. Revision of the Western Palaearctic Diplazontinae (Hymenoptera, Ichneumonidae). Zootaxa 3801, 1. https://doi.org/10.11646/zootaxa.3801.1.1

Kumar, S., Stecher, G., Tamura, K., 2016. MEGA7: Molecular Evolutionary Genetics Analysis Version 7.0 for Bigger Datasets. Mol. Biol. Evol. 33, 1870–1874. https://doi.org/10.1093/molbev/msw054

Lee, K.M., 2018. The demultiplexed fastq NCBI Sequence Read Archive (SAR) [WWW Document]. URL http://www.ncbi.nlm.nih.gov/sra/PRJNA505249

Lee, K.M., Kivelä, S.M., Ivanov, V., Hausmann, A., Kaila, L., Wahlberg, N., Mutanen, M., 2018. Information Dropout Patterns in Restriction Site Associated DNA Phylogenomics and a Comparison with Multilocus Sanger Data in a Species-Rich Moth Genus. Syst. Biol. 67, 925–939. https://doi.org/10.1093/sysbio/syy029

Leppänen, S. a., Altenhofer, E., Liston, A.D., Nyman, T., 2012. Phylogenetics and evolution of host-plant use in leaf-mining sawflies (Hymenoptera: Tenthredinidae: Heterarthrinae). Mol. Phylogenet. Evol. 64, 331–341. https://doi.org/10.1016/j.ympev.2012.04.005

Li, H., 2013. Aligning sequence reads, clone sequences and assembly contigs with BWA-MEM. arXiv 1303.3997.

Linnen, C.R., Farrell, B.D., 2008. Phylogenetic analysis of nuclear and mitochondrial genes reveals evolutionary relationships and mitochondrial introgression in the sertifer species group of the genus Neodiprion (Hymenoptera: Diprionidae). Mol. Phylogenet. Evol. 48, 240–57. https://doi.org/10.1016/j.ympev.2008.03.021

Linnen, C.R., Farrell, B.D., 2007. Mitonuclear discordance is caused by rampant mitochondrial introgression in Neodiprion (Hymenoptera: Diprionidae) sawflies. Evolution (N. Y). 61, 1417–38. https://doi.org/10.1111/j.1558-5646.2007.00114.x

Ma, Y., Zheng, B., Zhu, J., van Achterberg, C., Tang, P., Chen, X., 2019. The first two mitochondrial genomes of wood wasps (Hymenoptera: Symphyta): Novel gene rearrangements and higher-level phylogeny of the basal hymenopterans. Int. J. Biol. Macromol. 123, 1189–1196. https://doi.org/10.1016/j.ijbiomac.2018.11.017

Maddison, W.P., Maddison, D.R., 2017. Mesquite: a modular system for evolutionary analysis. Version 3.2.

Malm, T., Nyman, T., 2015. Phylogeny of the symphytan grade of Hymenoptera: New pieces into the old jigsaw(fly) puzzle. Cladistics 31, 1–17. https://doi.org/10.1111/cla.12069

Meier, R., Wong, W., Srivathsan, A., Foo, M., 2016. $1 DNA barcodes for reconstructing complex phenomes and finding rare species in specimen-rich samples. Cladistics 32, 100–110. https://doi.org/10.1111/cla.12115

Misof, B., Liu, S., Meusemann, K., Peters, R.S., Donath, A., Mayer, C., Frandsen, P.B., Ware, J., Flouri, T., Beutel, R.G., Niehuis, O., Petersen, M., Izquierdo-Carrasco, F., Wappler, T., Rust, J., Aberer, a. J., Aspock, U., Aspock, H., Bartel, D., Blanke, A., Berger, S., Bohm, A., Buckley, T.R., Calcott, B., Chen, J., Friedrich, F., Fukui, M., Fujita, M., Greve, C., Grobe, P., Gu, S., Huang, Y., Jermiin, L.S., Kawahara, a. Y., Krogmann, L., Kubiak, M., Lanfear, R., Letsch, H., Li, Y., Li, Z., Li, J., Lu, H., Machida, R., Mashimo, Y., Kapli, P., McKenna, D.D., Meng, G., Nakagaki, Y., Navarrete-Heredia, J.L., Ott, M., Ou, Y., Pass, G., Podsiadlowski, L., Pohl, H., von Reumont, B.M., Schutte, K., Sekiya, K., Shimizu, S., Slipinski, A., Stamatakis, A., Song, W., Su, X., Szucsich, N.U., Tan, M., Tan, X., Tang, M., Tang, J., Timelthaler, G., Tomizuka, S., Trautwein, M., Tong, X., Uchifune, T., Walzl, M.G., Wiegmann, B.M., Wilbrandt, J., Wipfler, B., Wong, T.K.F., Wu, Q., Wu, G., Xie, Y., Yang, S., Yang, Q., Yeates, D.K., Yoshizawa, K., Zhang, Q., Zhang, R., Zhang, W., Zhang, Y., Zhao, J., Zhou, C., Zhou, L., Ziesmann, T., Zou, S., Li, Y., Xu, X., Zhang, Y., Yang, H., Wang, J., Wang, J., Kjer, K.M., Zhou, X., 2014. Phylogenomics resolves the timing and pattern of insect evolution. Science (80-.). 346, 763–767. https://doi.org/10.1126/science.1257570

Mutanen, M., Kivelä, S.M., Vos, R.A., Doorenweerd, C., Ratnasingham, S., Hausmann, A., Huemer, P., Dincă, V., van Nieukerken, E.J., Lopez-Vaamonde, C., Vila, R., Aarvik, L., Decaëns, T., Efetov, K.A., Hebert, P.D.N., Johnsen, A., Karsholt, O., Pentinsaari, M., Rougerie, R., Segerer, A., Tarmann, G., Zahiri, R., Godfray, H.C.J., 2016. Species-Level Para- and Polyphyly in DNA Barcode Gene Trees: Strong Operational Bias in European Lepidoptera. Syst. Biol. 65, 1024–1040. https://doi.org/10.1093/sysbio/syw044

Niu, G., Korkmaz, E.M., Doğan, Ö., Zhang, Y., Aydemir, M.N., Budak, M., Du, S., Başıbüyük, H.H., Wei, M., 2019. The first mitogenomes of the superfamily Pamphilioidea (Hymenoptera:

Symphyta): Mitogenome architecture and phylogenetic inference. Int. J. Biol. Macromol. 124, 185–199. https://doi.org/10.1016/j.ijbiomac.2018.11.129
Normark, B.B., Jordal, B.H., Farrell, B.D., 1999. Origin of a haplodiploid beetle lineage. Proc. R. Soc. B Biol. Sci. 266, 2253–2259. https://doi.org/10.1098/rspb.1999.0916
Nyman, T., Zinovjev, A.G., Vikberg, V., Farrell, B.D., 2006. Molecular phylogeny of the sawfly subfamily Nematinae (Hymenoptera: Tenthredinidae). Syst. Entomol. 31, 569–583. https://doi.org/10.1111/j.1365-3113.2006.00336.x
Papakostas, S., Michaloudi, E., Proios, K., Brehm, M., Verhage, L., Rota, J., Peña, C., Stamou, G., Pritchard, V.L., Fontaneto, D., Declerck, S.A.J., 2016. Integrative Taxonomy Recognizes Evolutionary Units Despite Widespread Mitonuclear Discordance: Evidence from a Rotifer Cryptic Species Complex. Syst. Biol. 65, 508–524. https://doi.org/10.1093/sysbio/syw016
Paradis, E., Schliep, K., 2018. ape 5.0: an environment for modern phylogenetics and evolutionary analyses in R. Bioinformatics 1–3. https://doi.org/10.1093/bioinformatics/bty633
Patten, M.M., Carioscia, S.A., Linnen, C.R., 2015. Biased introgression of mitochondrial and nuclear genes: a comparison of diploid and haplodiploid systems. Mol. Ecol. 24, 5200–5210. https://doi.org/10.1111/mec.13318
Pentinsaari, M., Salmela, H., Mutanen, M., Roslin, T., 2016. Molecular evolution of a widely-adopted taxonomic marker (COI) across the animal tree of life. Sci. Rep. 6, 35275. https://doi.org/10.1038/srep35275
Pentinsaari, M., Vos, R., Mutanen, M., 2017. Algorithmic single-locus species delimitation: effects of sampling effort, variation and nonmonophyly in four methods and 1870 species of beetles. Mol. Ecol. Resour. 17, 393–404. https://doi.org/10.1111/1755-0998.12557
Peters, R.S., Krogmann, L., Mayer, C., Donath, A., Gunkel, S., Meusemann, K., Kozlov, A., Podsiadlowski, L., Petersen, M., Lanfear, R., Diez, P.A., Heraty, J., Kjer, K.M., Klopfstein, S., Meier, R., Polidori, C., Schmitt, T., Liu, S., Zhou, X., Wappler, T., Rust, J., Misof, B., Niehuis, O., 2017. Evolutionary History of the Hymenoptera. Curr. Biol. 27, 1013–1018. https://doi.org/10.1016/j.cub.2017.01.027
Peterson, B.K., Weber, J.N., Kay, E.H., Fisher, H.S., Hoekstra, H.E., 2012. Double Digest RADseq: An Inexpensive Method for De Novo SNP Discovery and Genotyping in Model and Non-Model Species. PLoS One 7, e37135. https://doi.org/10.1371/journal.pone.0037135
Philippe, H., Delsuc, F., Brinkmann, H., Lartillot, N., 2005. Phylogenomics. Annu. Rev. Ecol. Evol. Syst. 36, 541–562. https://doi.org/10.1146/annurev.ecolsys.35.112202.130205
Philippe, H., Vienne, D.M. de, Ranwez, V., Roure, B., Baurain, D., Delsuc, F., 2017. Pitfalls in supermatrix phylogenomics. Eur. J. Taxon. 283, 1–25. https://doi.org/10.5852/ejt.2017.283
Pritchard, J.K., Stephens, M., Donnelly, P., 2000. Inference of population structure using multilocus genotype data. Genetics 155, 945–59.
Prous, M., 2012. Taxonomy and phylogeny of the sawfly genus Empria (Hymenoptera, Tenthredinidae). Dissertationes biologicae universitatis tartuensis. Tartu Ülikooli Kirjastus.
Prous, M., Blank, S.M., Heibo, E., Lonnve, O.J., Vardal, H., Liston, A., 2014. Sawflies (Hymenoptera, Symphyta) newly recorded from Sweden. Entomol. Tidskr. 135, 135–146.
Prous, M., Heidemaa, M., Shinohara, A., Soon, V., 2011a. Review of the sawfly genus Empria (Hymenoptera, Tenthredinidae) in Japan. Zookeys 150, 347–380. https://doi.org/10.3897/zookeys.150.1968
Prous, M., Heidemaa, M., Soon, V., 2011b. Empria longicornis species group: taxonomic revision with notes on phylogeny and ecology (Hymenoptera, Tenthredinidae). Zootaxa 2756, 1–39. https://doi.org/10.11646/zootaxa.2756.1.1
Prous, M., Kramp, K., Vikberg, V., Liston, A., 2017. North-Western Palaearctic species of Pristiphora (Hymenoptera, Tenthredinidae). J. Hymenopt. Res. 59, 1–190. https://doi.org/10.3897/jhr.59.12656
Prous, M., Vikberg, V., Liston, A., Kramp, K., 2016. North-Western Palaearctic species of the

Pristiphora ruficornis group (Hymenoptera, Tenthredinidae). J. Hymenopt. Res. 51, 1–54. https://doi.org/10.3897/jhr.51.9162

R Core Team, 2017. R: A language and environment for statistical computing.

Rambaut, A., 2015. FigTree, v1.4.2: Tree Figure Drawing Tool. Molecular evolution, phylogenetics and epidemiology. Available from: http://tree.bio.ed.ac.uk/software/figtree/.

Rosenberg, N.A., 2004. distruct: a program for the graphical display of population structure. Mol. Ecol. Notes 4, 137–138. https://doi.org/10.1046/j.1471-8286.2003.00566.x

Roux, C., Fraïsse, C., Romiguier, J., Anciaux, Y., Galtier, N., Bierne, N., 2016. Shedding Light on the Grey Zone of Speciation along a Continuum of Genomic Divergence. PLOS Biol. 14, e2000234. https://doi.org/10.1371/journal.pbio.2000234

Schmidt, S., Schmid-Egger, C., Morinière, J., Haszprunar, G., Hebert, P.D.N., 2015. DNA barcoding largely supports 250 years of classical taxonomy: identifications for Central European bees (Hymenoptera, Apoidea partim). Mol. Ecol. Resour. 15, 985–1000. https://doi.org/10.1111/1755-0998.12363

Schmidt, S., Taeger, A., Morinière, J., Liston, A., Blank, S.M., Kramp, K., Kraus, M., Schmidt, O., Heibo, E., Prous, M., Nyman, T., Malm, T., Stahlhut, J., 2017. Identification of sawflies and horntails (Hymenoptera, 'Symphyta') through DNA barcodes: successes and caveats. Mol. Ecol. Resour. 17, 670–685. https://doi.org/10.1111/1755-0998.12614

Schnell, I.B., Bohmann, K., Gilbert, M.T.P., 2015. Tag jumps illuminated - reducing sequence-to-sample misidentifications in metabarcoding studies. Mol. Ecol. Resour. 15, 1289–1303. https://doi.org/10.1111/1755-0998.12402

Simion, P., Philippe, H., Baurain, D., Jager, M., Richter, D.J., Di Franco, A., Roure, B., Satoh, N., Quéinnec, É., Ereskovsky, A., Lapébie, P., Corre, E., Delsuc, F., King, N., Wörheide, G., Manuel, M., 2017. A Large and Consistent Phylogenomic Dataset Supports Sponges as the Sister Group to All Other Animals. Curr. Biol. 27, 958–967. https://doi.org/10.1016/j.cub.2017.02.031

Sloan, D.B., Havird, J.C., Sharbrough, J., 2017. The on-again, off-again relationship between mitochondrial genomes and species boundaries. Mol. Ecol. 2212–2236. https://doi.org/10.1111/mec.13959

Stamatakis, A., 2014. RAxML version 8: a tool for phylogenetic analysis and post-analysis of large phylogenies. Bioinformatics 30, 1312–1313. https://doi.org/10.1093/bioinformatics/btu033

Swofford, D.L., 2003. PAUP*: phylogenetic analysis using parsimony, version 4.0 b10. Sinauer Associates, Sunderland, MA.

Taeger, A., Liston, A.D., Prous, M., Groll, E.K., Gehroldt, T., M., B.S., 2018. ECatSym – Electronic World Catalog of Symphyta (Insecta, Hymenoptera). Program version 5.0 (19 Dec 2018), data version 40 (23 Sep 2018) [WWW Document]. URL https://sdei.de/ecatsym/

Tamura, K., Stecher, G., Peterson, D., Filipski, A., Kumar, S., 2013. MEGA6: Molecular Evolutionary Genetics Analysis version 6.0. Mol. Biol. Evol. 30, 2725–2729. https://doi.org/10.1093/molbev/mst197

Tang, P., Zhu, J., Zheng, B., Wei, S., Sharkey, M., Chen, X., Vogler, A.P., 2019. Mitochondrial phylogenomics of the Hymenoptera. Mol. Phylogenet. Evol. 131, 8–18. https://doi.org/10.1016/j.ympev.2018.10.040

Tang, Q.-Y., Liu, S.-Q., Yu, D., Liu, H.-Z., Danley, P.D., 2012. Mitochondrial capture and incomplete lineage sorting in the diversification of balitorine loaches (Cypriniformes, Balitoridae) revealed by mitochondrial and nuclear genes. Zool. Scr. 41, 233–247. https://doi.org/10.1111/j.1463-6409.2011.00530.x

Tarver, J.E., dos Reis, M., Mirarab, S., Moran, R.J., Parker, S., O'Reilly, J.E., King, B.L., O'Connell, M.J., Asher, R.J., Warnow, T., Peterson, K.J., Donoghue, P.C.J., Pisani, D., 2016. The Interrelationships of Placental Mammals and the Limits of Phylogenetic Inference. Genome Biol. Evol. 8, 330–344. https://doi.org/10.1093/gbe/evv261

van der Valk, T., Vezzi, F., Ormestad, M., Dalén, L., Guschanski, K., 2019. Index hopping on the Illumina HiseqX platform and its consequences for ancient DNA studies. Mol. Ecol. Resour. 179028, 1755–0998.13009. https://doi.org/10.1111/1755-0998.13009

Zahiri, R., Lafontaine, J.D., Schmidt, B.C., DeWaard, J.R., Zakharov, E. V., Hebert, P.D.N., 2017. Probing planetary biodiversity with DNA barcodes: The Noctuoidea of North America. PLoS One 12, e0178548. https://doi.org/10.1371/journal.pone.0178548

[Figures and figure captions]

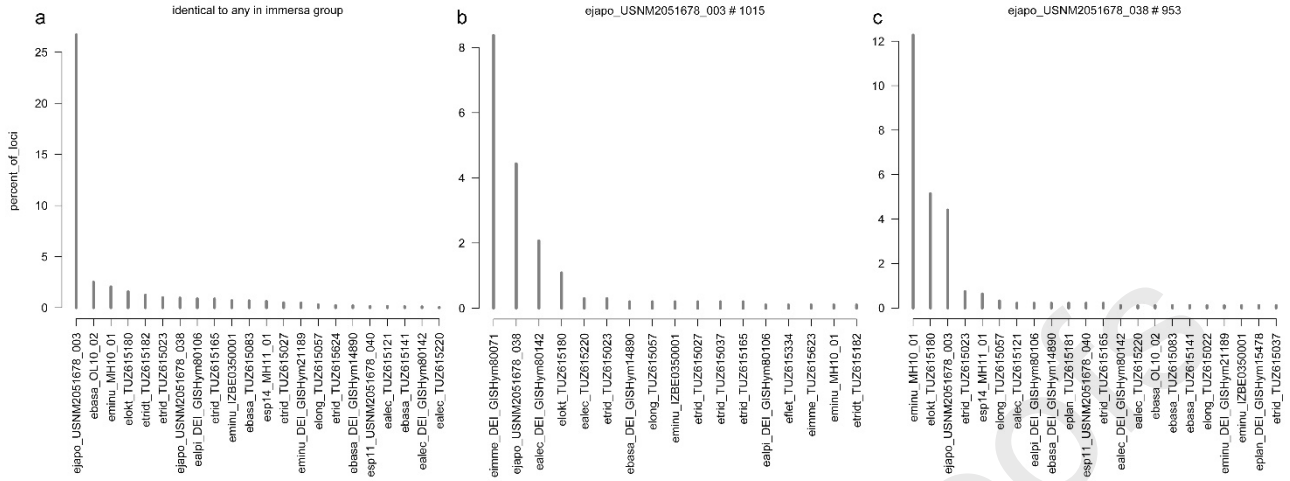

Fig. 1. Examples of results of cross-contamination check by counting identical loci among *Empria* specimens (dataset with 19 413 loci, Supplementary Data S4). For results of all samples see Supplementary Data S5. (a) Percent of loci in every *longicornis* group specimen (X-axis) (including *E. tridentis*) that are identical to any specimen in the *immersa* group, while different from other specimens in the *longicornis* group (if present). (b, c) Percent of loci in *E. japonica* USNM2051678_003 (b) and USNM2051678_038 (c) that are identical to a particular specimen (listed along X-axis) while different from the others in the dataset.

(a) *E. longicornis* group

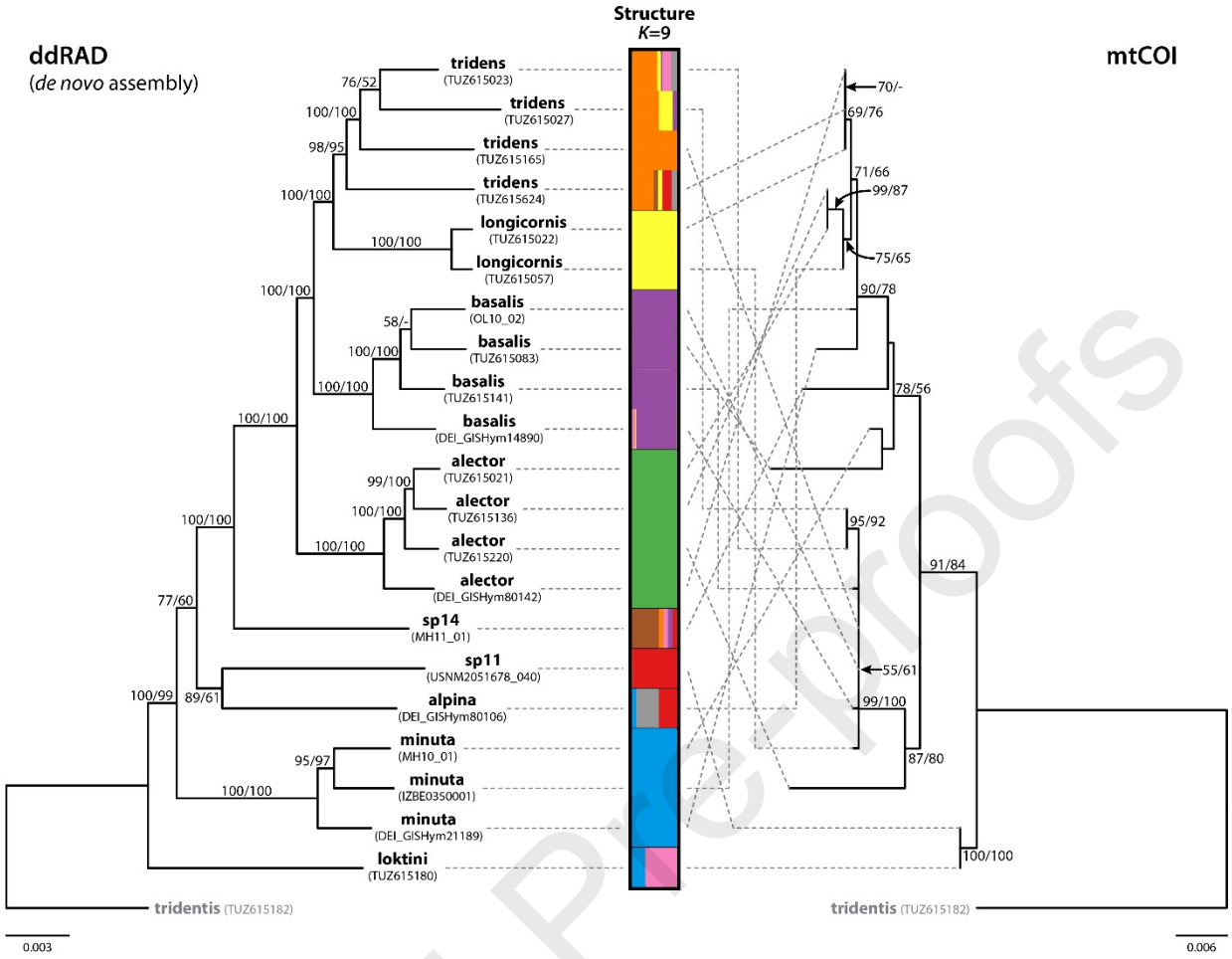

(b) *E. immersa* group

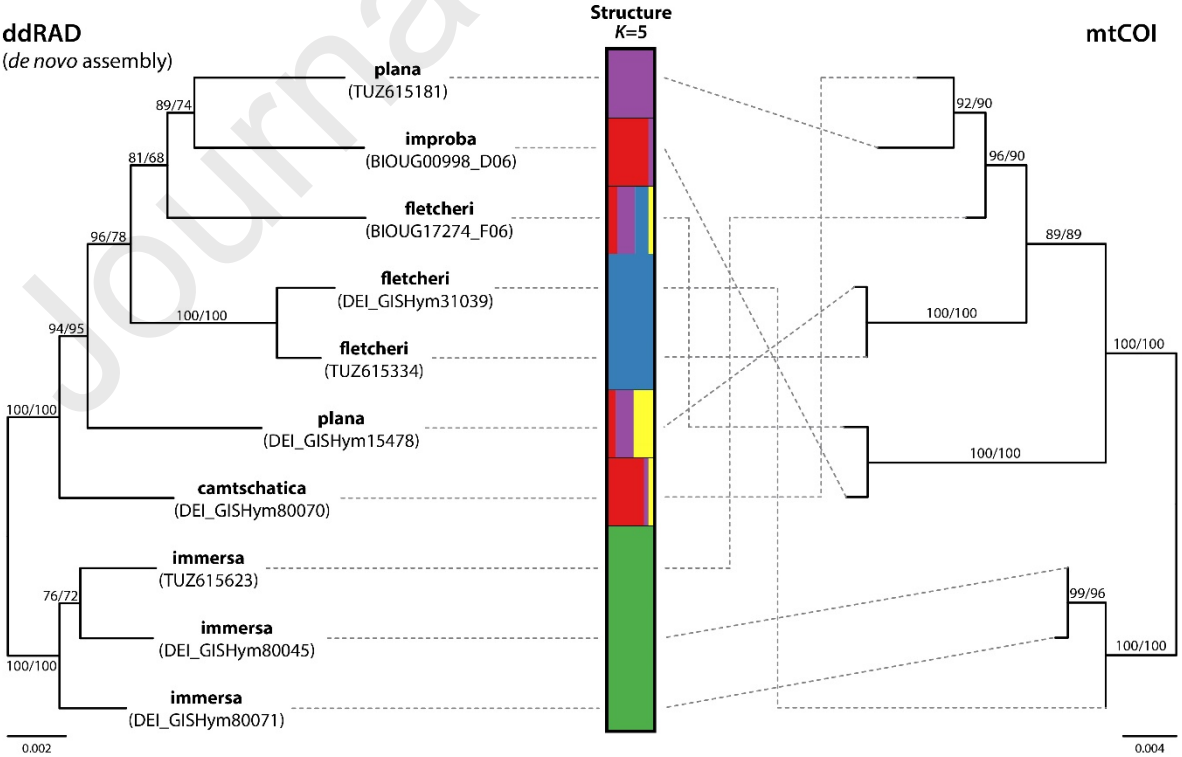

Fig. 2. Maximum likelihood trees of two *Empria* species groups and population admixture analyses based on ddRAD *de novo* assemblies in comparison with mitochondrial COI maximum likelihood tree (1536 bp). (a) *E. longicornis* group (ddRAD dataset with 20 871 loci). (b) *E. immersa* group (ddRAD dataset with 9 362 loci). Bootstrap support values (%) below or above branches resulting from maximum likelihood (ML) and maximum parsimony (MP) analyses are shown as ML/MP.

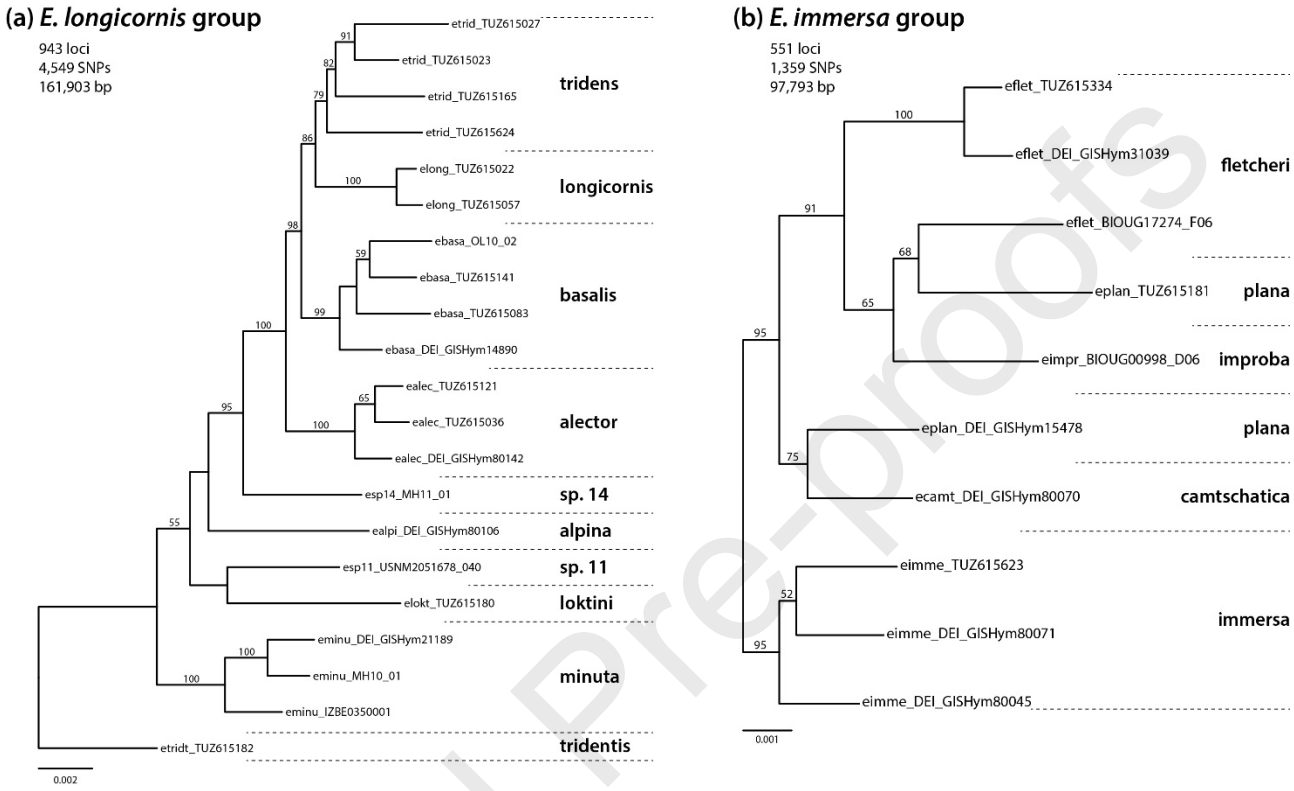

Fig. 3. Maximum likelihood trees of two *Empria* species groups based on ddRAD reference assembly. (a) *E. longicornis* group. (b) *E. immersa* group.

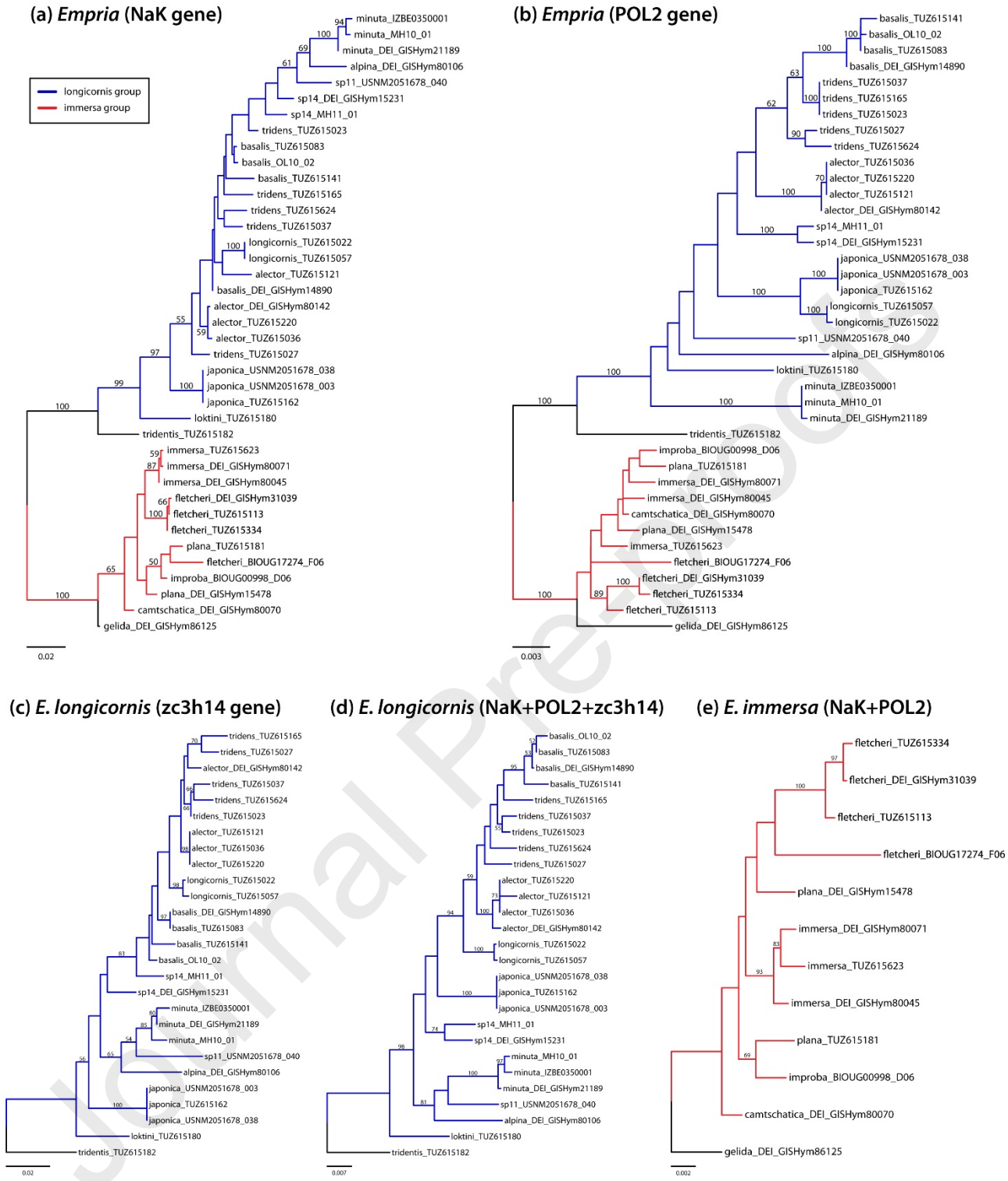

Fig. 4. Maximum likelihood trees based on three nuclear protein coding genes obtained by Sanger sequencing. (a) NaK (1654 bp). (b) POL2 (2494 bp). (c) ZC3H14 (alignment 1654 bp). (d) Concatenated NaK, POL2, and ZC3H14 (alignment 5802 bp) for *longicornis* group. (e) Concatenated NaK and POL2 (4148 bp) for *immersa* group.

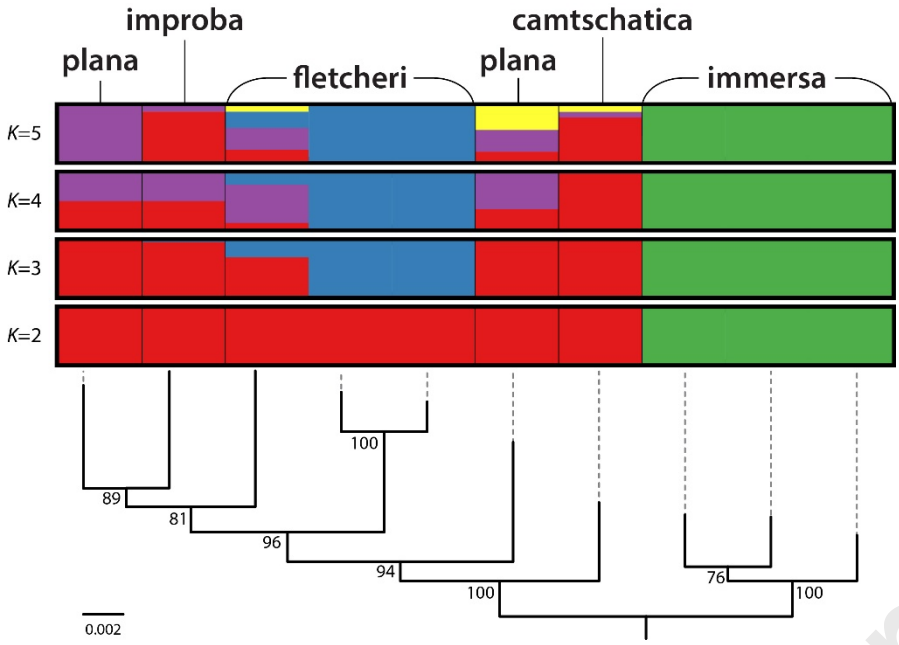

Fig. 5. Population admixture analysis of *Empria immersa* group with Structure at *K*=3 to *K*=5 (*de novo* assembly). Maximum likelihood tree from Fig. 2 is shown below the results of Structure analyses.

Graphical abstract

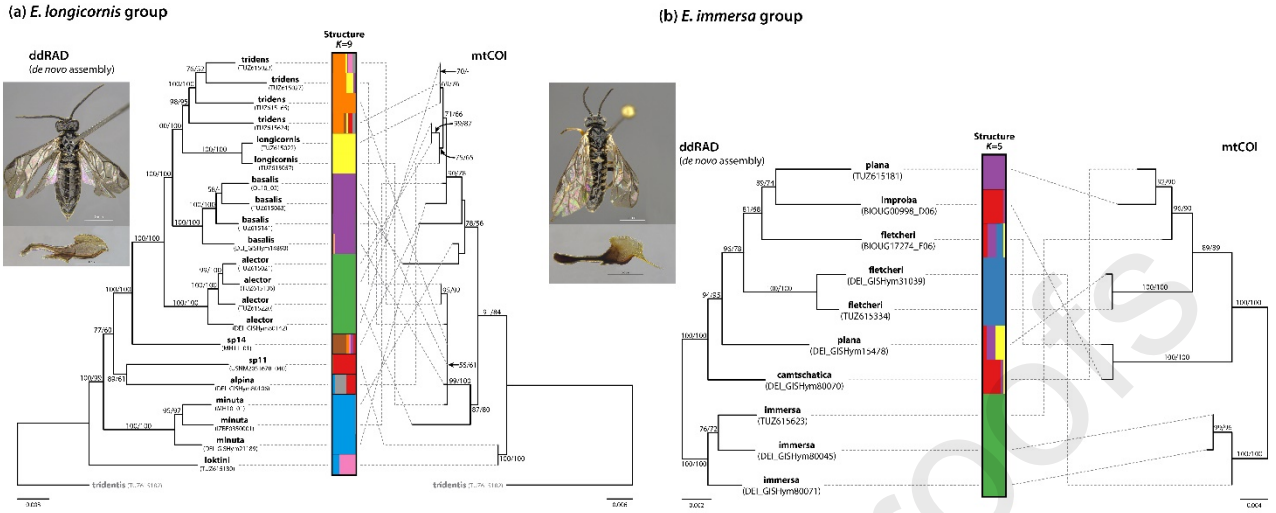

Highlights

Two specimens of *E. japonica* were apparently substantially more cross-contaminated than other specimens (possibly 10–20% of recovered loci) and were excluded from further analyses

An R script is provided to examine patterns of identical loci among specimens in ddRAD data

Analyses of ddRAD data and Sanger sequencing of two to three nuclear protein coding genes revealed strong discordance with mitochondrial phylogeny within two species groups of *Empria*

Taxonomy of *E. longicornis* group was well and taxonomy of *E. immersa* group moderately supported by nuclear (ddRAD and Sanger) data, but not by mitochondrial COI sequences